Cell-Specific Ca^{2+} Response In Pancreatic ß-Cells

Natalia Gustavsson

Department of Integrative Medical Biology,
Section for Histology and Cell biology
Umeå University
Umeå 2006

To my Family

CONTENTS

ABSTRACT

Pancreatic ß-cells are heterogeneous in many respects, including their secretory responsiveness, glucose sensitivity and metabolic rate. We do not know precisely which mechanisms control functional characteristics, such as time of insulin release (lag-time) or magnitude of the response in each individual cell or islet. The heterogeneity might represent a random phenomenon or could be a manifestation of constant characteristics inherent to individual ß-cells. This is an important question because a diminished and delayed first-phase insulin release is an early sign of failing ß-cells.

We compared lag-times, initial lowering nadirs and first $[Ca^{2+}]_i$ peak heights in Fura-2 loaded *ob/ob* mouse ß-cells during two consecutive stimulations with glucose. There was a strong correlation of corresponding parameters between the first and second stimulation. Thus, timing and magnitude of the early Ca^{2+} response were individual and reproducible characteristics in ß-cells. We then studied Ca^{2+} responses in ß-cells from lean mice, diabetic *db/db* mice and rats stimulated twice with 20 mM glucose and found cell-specific response characteristics also in those cells. This indicates that a cell-specific Ca^{2+} response to glucose is common in rodent ß-cells, both normal and diabetic. Another question was whether aggregated ß-cells show cell-specific responses. Using the same protocol as for dispersed ß-cells, we analysed Ca^{2+} responses in single *ob/ob* mouse ß-cells within a small cluster (3-7 cells), in clusters of medium (about 10 cells) and large size (about 25 cells) and also in intact islets from *ob/ob* and lean mice. Significant correlations were found between the first and second stimulation for timing and magnitude of $[Ca^{2+}]_i$ rise, and for initial lowering.

Next, we tested if the ß-cell response is cell-specific, when induced at different steps of stimulus-secretion coupling. The glycolytic intermediate glyceraldehyde, the mitochondrial substrate KIC, the K_{ATP}-channel blocker tolbutamide and arginine were used as tools. $[Ca^{2+}]_i$ changes were studied in dispersed ß-cells from lean, *ob/ob* and *db/db* mice. NAD(P)H responses to glucose and KIC were analyzed as a measure of metabolic flux. With regard to the cell specificity, the correlation between Ca^{2+} and insulin response from individual ß-cells was studied using the calcium dye Fluo-3 and Fluozin-3, which is a probe for Zn^{2+}, co-released with insulin. Both timing and magnitude of calcium responses were cell-specific in lean mouse ß-cells with all tested secretagogues. ß-Cells from *ob/ob* and *db/db* mice showed cell-specific temporal Ca^{2+} responses to glyceraldehyde but not to KIC. The lag-time for the Ca^{2+} response to KIC was shorter during the second stimulation in ß-cells from hyperglycemic mice. Tolbutamide and arginine induced no cell-specific temporal Ca^{2+} response in dispersed *ob/ob* and *db/db* mouse ß-cells. However, the timing of tolbutamide-induced response was cell-specific in *ob/ob* mouse ß-cells within intact islets. NAD(P)H changes to glucose were cell-specific in all three mouse models, but the timing of NAD(P)H response to KIC was cell-specific only in lean mice. Thus, a cell-specific response can be induced in normal ß-cells at several steps of stimulus-secretion coupling for nutrient-stimulated insulin release. Mitochondrial metabolism generates a cell-specific temporal response in ß-cells from lean but not from *db/db* and *ob/ob* mice. Cell-specific properties of ß-cell ion channels also seem to be affected in these mice.

The relation between mitochondrial mass and parameters of Ca^{2+} responses were investigated in Mitotracker Red and Fluo-3 labelled ß-cells using confocal microscopy. Data show that ß-cell mitochondrial status may play an important role in determining the timing of $[Ca^{2+}]_i$ changes.

In summary, the early Ca^{2+} response pattern, including the lag-time, the nadir of initial lowering and the height of the first peak response is cell-specific in ß-cells. Isolated and functionally coupled ß-cells show cell-specific timing of Ca^{2+} responses when stimulated with metabolic and non-metabolic agents. This may be a robust mechanism of importance for the adequate function of ß-cells and a basis for the pacemaker function of some cells. A disturbed cell specificity of the mitochondrial metabolism appears to be a marker of ß-cell dysfunction in hyperglycemia and diabetes and may explain the delayed insulin release in ß-cells from diabetic subjects. Early steps in glucose metabolism seem to be less vulnerable in this regard.

ORIGINAL PAPERS

This thesis is based on the following papers, which are referred to in the text by their Roman numerals:

I. Gerd Larsson-Nyrén, Natalia Pakhtusova and Janove Sehlin (2002) Isolated mouse pancreatic β-cells show cell-specific temporal response pattern. Am. J. Physiol., 282, C1199-C1204.

II. Natalia Pakhtusova, Lidia Zaostrovskaya, Per Lindström and Gerd Larsson-Nyrén (2003) Cell-specific Ca^{2+} responses in glucose-stimulated single and aggregated ß-cells. Cell Calcium, 365, 1-9.

III. Natalia Gustavsson, Gerd Larsson-Nyrén and Per Lindström. Pancreatic ß-cells from *db/db* mice show cell-specific $[Ca^{2+}]_i$ and NADH responses to glucose but not to alpha-ketoisocaproic acid. Pancreas, 31(3), 242-50.

IV. Natalia Gustavsson, Gerd Larsson-Nyrén and Per Lindström. (Manuscript) Cell specificity of Ca^{2+} response to tolbutamide is impaired in ß-cells from hyperglycemic mice.

V. Natalia Gustavsson, Golbarg Abedi, Gerd Larsson-Nyrén and Per Lindström. (Manuscript) Timing of Ca^{2+} response in pancreatic ß-cells is related to mitochondrial mass.

ABBREVIATIONS

BSA	bovine serum albumin
$[Ca^{2+}]_i$	cytoplasmic calcium concentration
CoA and acetyl-CoA	coenzyme A and its acyl derivative
cAMP	cyclic adenosine 3' : 5'-monophosphat
DNAase	deoxyribonuclease
EDTA	ethylene diamine tetraacetic acid
IP_3	inositol 1,4,5-trisphosphate
DIC	differential interference contrast
CCD	charge-coupled device
K_{ATP}-channels	ATP-sensitive potassium channels
KIC	α-ketoisocaproic acid
SUR1	sulfonylurea receptor 1
TPEN	tetrakis(2-pyridylmethyl)ethylenediamine

INTRODUCTION

Blood sugar control in mammals is dependent on secretion of hormones from the islets of Langerhans, principally insulin. Pancreatic ß-cells measure extracellular glucose concentrations with a high degree of sensitivity and rapidly release insulin in response to a rise in the glucose level. Although the release of insulin is mostly regulated by the glucose level in the plasma, many other nutrients, hormones and neural stimuli can modulate the release. Impairment of the action of insulin causes metabolic disorders, such as glucose intolerance and diabetes. A combination of reduced peripheral insulin sensitivity and ß-cell dysfunction characterises type 2 diabetes (non-insulin-dependent diabetes mellitus) (for review Nadal 1999), responsible for 90-95% of all diabetic cases. This disease is associated with disturbances in the insulin release pattern, i.e. a selective loss of first phase secretion, which precedes the other manifestations (Cerasi and Luft 1967), and impairment of the pulsatile rhythm of secretion (Bergsten 2000). The insulin secretory response of type 2-diabetic patients is delayed and decreased (Cerasi et al 1972, Calles-Escandon and Robbins 1987, Polonsky et al 1998). For understanding of the pathogenesis of type 2 diabetes and for development of effective treatment, it is crucial to have knowledge of the mechanisms regulating normal insulin secretion, including the control of the individual ß-cell responsiveness.

The structure of a pancreatic islet

Pancreatic islets are mainly composed of insulin-producing ß-cells (65-90% in different species), which in most mammals are located in the central part of the islets and surrounded by other hormone-producing cells (Hellerström *et al* 1960, Pipeleers 1987). Other cell types are glucagon-releasing α-cells, somatostatin-producing δ-cells and pancreatic polypeptide-producing PP-cells, as well as some other rare cell types. Gap junctions connect different ß-cells (Orci *et al* 1973, Int Veld *et al* 1986) as well as ß-cells and other endocrine islet cells, providing a pathway for the cell-to-cell diffusion of hydrophilic molecules, such as ions, metabolites and second messengers (for review Munari-Silem and Rousset 1996). There is evidence that the ß-cells in intact islets are functionally coupled and show synchronised activity (Perez-Armendariz *et al* 1995).

Stimulus-secretion coupling in ß-cells

Metabolic signals play an important role in the sequence of cellular events resulting in insulin release during stimulation with glucose and other nutrient secretagogues (Newgard and McGarry 1995, Matschinsky 1996, Tamarit-Rodriguez *et al* 1998) (Figure 1). Glucose enters through the GLUT transporter (Figure 1). The glucokinase and phosphofructokinase steps are important for the regulation of glycolysis (for review Deeney *et al* 2000). One of the intermediate glycolytic metabolites is glyceraldehyde phosphate. For experimental purposes glyceraldehyde is often used to by-pass early glycolytic steps. It enters the glycolytic pathway via its phosphorylation by ATP to form glyceraldehyde phosphate. The subsequent metabolism of glyceraldehyde is identical to that of glucose (Figure 1), i.e. metabolised further through glycolysis generating pyruvate and reduced pyridine nucleotides.
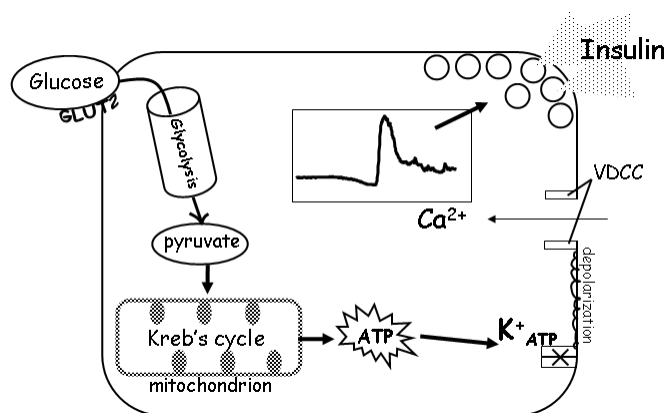
Figure 1. Scheme of glucose-induced insulin release. Abbreviations used are: GLUT2, glucose transporter type 2; K^+_{ATP}, ATP-sensitive potassium channels; VDCC, voltage-dependent calcium channels.

Pyruvate undergoes metabolism in the mitochondria and the nucleotides are reoxidised through mitochondrial NADH shuttle systems. An essential step in the stimulus-secretion coupling cascade is ATP production and a change in ATP/ADP ratio. ATP is produced both during glycolysis in the cytoplasm and through oxidative phosphorylation that takes place in mitochondria during the breakdown of pyruvate. α-Ketoisocaproic acid (KIC) can be used to increase mitochondrial metabolism (Fig. 1). KIC is a transamination partner for glutamic acid or glutamine to yield α-ketoglutarate and leucine (Lembert and Idahl 1998). Glucose also increases the production of cytosolic NADH and the reducing equivalents are transported into the mitochondria by the α-glycerolphosphate and malate/aspartate shuttles for rapid ATP synthesis. The rise in ATP-ADP ratio (and, perhaps, other signals) results in closure of ATP-sensitive K channels (K_{ATP}-channels) in the plasma membrane and a depolarisation of the ß-cell. Voltage-dependent Ca^{2+}

channels open and the cytoplasmic free Ca^{2+} level rises, triggering insulin exocytosis (for review, Dunne and Petersen 1991, Misler *et al* 1992).

Influencing K_{ATP}-channels with synthetic drugs can also stimulate insulin secretion. Sulfonylureas, which are used for treatment of type-2 diabetic patients, bind to sulfonylurea receptors (SUR1) (Ashcroft and Ashcroft 1992) and in this way block potassium channels (Trube *et al*, 1986). Sulfonylureas induce a peak of insulin release often followed by a stable period of secretion at a lower rate (Grodsky *et al* 1969). However, they do not stimulate insulin biosynthesis and even inhibit glucose-stimulated biosynthetic activity in ß-cells (Shatz *et al* 1972, Levy and Malaisse 1975). Arginine directly causes ß-cell depolarisation, similarly to cations (Charles *et al* 1982, Herchuelz *et al* 1984). In diabetic subjects, the response to sulfonylureas and arginine is less impaired than the response to glucose (Del Guerra *et al*, 2005).

Glucose-induced insulin secretion is biphasic. There is a transient first phase lasting 5–10 min, which is then followed by a sustained second phase (Curry *et al*, 1968).

The effect of ß-cell secretagogues is not limited to the acute stimulation of insulin release. As an example, glucose may either desensitise or sensitise the islet to subsequent stimulations depending on concentration and duration of the stimulation (Curry *et al* 1968, Nesher *et al* 1989). The terms "time-dependent inhibition" (TDI) and "time-dependent potentiation" (TDP) have been suggested to describe these effects since they require a certain duration of exposure to the stimulatory agent (Nesher *et al* 1989). These effects seem to operate through a memory induced in the stimulus-secretion pathway and persist after the removal of the stimulator from the medium. Glucose metabolism (Grill *et al*, 1978) and intracellular pH regulation (Gunawardana and Sharp 2002) may be important cellular mechanisms causing time-dependent effects.

Ca^{2+} response in ß-cells

Glucose induces a triphasic Ca^{2+} response in ß-cells (for review Gilon *et al* 1994). As Fig. 2 shows, a small initial decrease is followed by a large peak increase in $[Ca^{2+}]_i$ (Nilsson *et al* 1988, Gylfe 1989). The initial lowering is caused by sequestration of intracellular Ca^{2+} to the intracellular pool and is regulated by glucose metabolism (Lund *et al* 1989). After the peak, $[Ca^{2+}]_i$ usually remains increased for as long as the stimulation lasts, and often in the form of oscillations. The timing and magnitude of calcium response are important regulatory factors
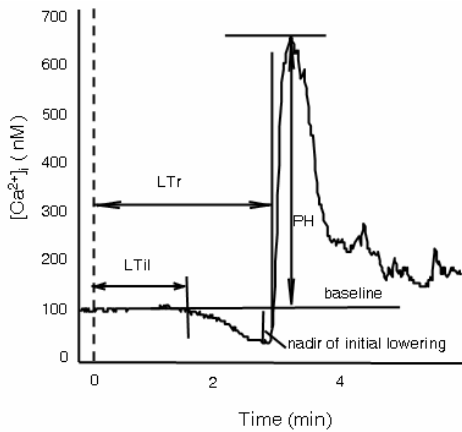
Figure 2.
(Figure 1 in paper 3) Schematic presentation of Ca^{2+} response with analysed variables: lag-time for initial lowering (LTil), nadir of initial lowering, lag-time for $[Ca^{2+}]_i$ rise (LTr), and peak height (PH) in single ß-cells. Test medium is added at time 0 min

because of the close temporal and quantitative relationships between $[Ca^{2+}]_i$ and insulin secretion patterns (Bergsten *et al* 1994, Jonas *et al* 1998). As for insulin release, the Ca^{2+} response to glucose is decreased and delayed in diabetic animal ß-cells (Lindström *et al* 1996).

Heterogeneity concept

The heterogeneity among pancreatic ß-cells is well documented (Salomon and Meda 1986, Herchuelz *et al* 1991, Van Schravendijk *et al* 1992). Individual ß-cells show different amounts of secretory granules and rough endoplasmic reticulum (Stefan *et al* 1987) and number of gap junctions (Meda *et al*, 1980). ß-Cells differ in their glucose sensitivity (Kiekens *et al* 1992) and biosynthetic (Schuit *et al* 1988) and secretory (Hiriart and Ramirez-Medeles 1991, Pipeleers *et al* 1994) capabilities. A marked heterogeneity has been noted in the electrical activity among ß-cells (Dunne 1990, Kinard *et al* 1999) and Ca^{2+} response pattern (Pralong *et al* 1990, Gylfe *et al* 1991, Herchuelz *et al* 1991, Larsson-Nyrén and Sehlin 1996). Heterogeneity of secretory and electrophysiological responses was found also in intact islets (Aizawa *et al* 2001). Despite the large number of studies performed on ß-cells, the mechanisms underlying functional heterogeneity among pancreatic ß-cells are not known. Some evidence suggests that intercellular differences in glucose metabolism and K_{ATP}-channel currents are important (Faehling and Ashcroft 1997, Schiut *et al* 1997). In most of the studies showing heterogeneity in the ß-cell population, ß-cells were stimulated only once with glucose and the observations were made using unpurified islet cell preparations. These studies have demonstrated group differences but they have not addressed the question of whether different functional characteristics of ß-cells within the population reflect inherent qualities of ß-cells or random phenomena. Knowledge of the mechanisms determining timing of response in individual ß-cells is

important in view of the fact that the first phase of insulin secretion is impaired already in early stages of type 2 diabetes (Cerasi *et al* 1972).

Hyperglycemic ob/ob and db/db mice

The *ob/ob* mouse mutation was first recognised in 1949 at the Jackson Memorial Laboratory, Bar Harbor, USA (Ingalls et al 1950) and was bred into several mouse sublines (e.g. Umeå *ob/ob* mouse). The *ob/ob* syndrome is caused by hyperphagia due to a genetic defect of leptin, a satiety factor that regulates the balance of food intake and consumption (Halaas et al 1995). Characteristic features of this mouse mutation are obesity, hyperinsulinemia and mild hyperglycemia (Stauffacher *et al* 1967, Stauffacher and Renold 1969). However, these animals do not develop overt diabetes with ketosis (Hunt *et al* 1976). Islets from *ob/ob* mice respond normally to stimulators of insulin release (Hahn *et al* 1974, Hellman *et al* 1974). One advantage of using Umeå *ob/ob* mice is the very high proportion of ß cells in their pancreatic islets (>90%) (Hellman 1965). Another hyperglycemic animal model is the *db/db* mouse (Hunt *et at* 1976). These mice lack functional leptin receptors (Chen *et al* 1996). Within 6 weeks of age, they develop a severe diabetic syndrome, characterised by obesity, fasting hyperglycemia, glycosuria, and hyperinsulinemia (Berglund *et al* 1978). Their ß-cells show a defective Ca^{2+} response to glucose stimulation (Roe *et al* 1994).

AIMS OF THE PRESENT THESIS WORK

✓ To determine whether the functional heterogeneity of calcium responses among ß-cells represents a cell-specific, inherent quality of pancreatic ß-cells or a random phenomenon.

✓ To find out if a cell-specific response can be observed in ß-cells from different animal models, in ß-cell clusters and intact pancreatic islets.

✓ To determine if Ca^{2+} responses are cell-specific when induced at different steps of the stimulus-secretion coupling.

✓ To test whether the pattern of cell specificity of ß-cell response is different in obesity and diabetes.

✓ To investigate if there is a correlation between the mitochondrial mass and the timing and magnitude of calcium response.

MATERIALS AND METHODS

Animals

Pancreatic islets were obtained from non-inbred, 7- to 8-mo-old female *ob/ob* mice and their lean littermates (Umeå-*ob/ob*), and adult female rats (Sprague–Dawley, 200–250 g). *db/db* Mice (BKS.Cg-m+/+Lepr[db]) were from Taconic Europe, Ry, Denmark. They were brought to our animal care facility at the age of 6 weeks and were housed until 3-4 months. For experiment series where *db/db* and lean mice were compared, lean mice were 4-5-mo-old. Principles of laboratory animal care (NIH publication no. 83-25, revised 1985) were followed and the animal care and experimental procedures were carried out in accordance with the standards established by the European Communities Council Directive (86/609/EEC9). The experiments were also approved by the Northern Swedish Committee for Ethics in Animal Experiments.

In overnight fasted *db/db* mice the blood sugar level was 22 ± 2 mM (mean $\pm$ S.D., N=33). The urinary glucose level was 17 ± 2 mM (N=33). The body weight was 50 ± 1 g (N=33). The body weight of *ob/ob* mice was 73 ± 2 g (N=16). The blood sugar in overnight fasted *ob/ob* mice was 7 ± 0.4 mM (N=16), with negative urinary glucose. The body weight of lean mice was 24 ± 1 g (N=15) and the blood sugar level was 5 ± 0.4 mM (N=15). (Data from Paper IV).

Islet and ß-cell preparation

Isolated mouse islets from *db/db* mice, *ob/ob* mice and their lean littermates were obtained by collagenase digestion. Single *ob/ob* and *db/db* mouse ß-cells were prepared by shaking the isolated islets in a Ca^{2+}-deficient medium supplemented with EGTA and DNAase (Lernmark 1974). Single lean mouse ß-cells were obtained by digestion with 0.025 mg/ml trypsin and 50 µl/ml DNAase. The cells were distributed on polylysine-coated cover glasses placed in Petri dishes and maintained in tissue culture for 24-48 hours in RPMI 1640 medium supplemented with 10% heat-inactivated fetal calf serum, 60 mg/ml garamycin, 60 mg/ml benzylpenicillin and 2 mM L-glutamine. Subsequent experimental handling was performed in a Krebs-Ringer medium (KRH) having the following composition in mM: 130 NaCl, 4.7 KCl, 1.2 KH_2PO_4, 1.2 $MgSO_4$, and 2.56 $CaCl_2$ and supplemented with 1mg/ml BSA and 3 mM D-glucose. The medium was buffered with 20 mM HEPES and NaOH to reach pH 7.4 and equilibrated with ambient air. Isolation of rat islets was performed by infiltrating the pancreata with 2.0 mg/ml collagenase via the main pancreatic duct system. The isolated islets were obtained by shaking the pancreas at 37° C. Preparation and culture of rat ß-cells was performed as described for the *ob/ob* mouse ß-cells.

Measurements of cytoplasmic Ca^{2+} with Fura-2

Cells and islets were loaded with 1µM Fura-2 for 40 min in KRH medium at 37°C. After rinsing in KRH to remove extracellular Fura-2, the cover glasses were mounted as the bottom of an open chamber and placed on the stage of an inverted microscope within a climate box maintained at 37° C. Three microscope systems were used: Nikon

Diaphot-TMD (Bimica), Zeiss IM and Zeiss Axiovert. We have previously found that absolute values for $[Ca^{2+}]_i$ may differ slightly when measured in the three microscope systems, but the recorded response pattern is similar. Because of this difference, absolute $[Ca^{2+}]_i$ values were not compared between sets of experiments performed on different microscopes. The cells and islets were continuously superfused at a flow rate of 0.6 ml/min. The Fura-2 signal was successively excited at the wavelengths 340 and 380 nm with band-pass filters in front of a 75-watt xenon lamp. Using Nikon or Zeiss IM, the resulting emitted fluorescence was measured with a photomultiplier at 510 nm. In experiments, performed on Zeiss Axiovert, an image analysis system Openlab 3 (Improvision, Coventry, UK) was used. Fura-2 was successively excited at the wavelengths 340 and 380 nm during 23 ms each using a 75-watt xenon lamp and a Polychrome IV monochromator (TILL Photonics, Germany). Images were acquired by a CCD camera (Orca ER, Hamamatsu, Japan). The interval between successive cycles of 340/380 nm excitation was 1.26 s or 1.75 s (Nikon and Zeiss Axiovert) or 5 s (Zeiss IM). $[Ca^{2+}]_i$ was calculated from the ratio of 340 nm and 380 nm signals after background subtraction using the equation described by Grynkiewicz $et\ al$ (1985), with a K_d of 224 nM.

Measurements of cytoplasmic Ca^{2+} with Fluo-3

Experiments were performed using the Leica SP2 spectral laser scanning confocal microscopy system (Leica Microsystems, Mannheim, Germany). Intact islets were labelled with the calcium dye Fluo-3 and placed on coverslips on the bottom of an open perifusion chamber. The chamber was put on the stage of the microscope and maintained at 37°C. Islets were continuously superfused at a flow rate of 0.6 ml/min. Cells were first visualized using transmission laser scanning microscopy. Fluo-3 was excited with the 488-nm line of an argon laser. Fluo-3 responses were recorded from peripheral cells in one randomly chosen cross-section in islets using a Leica ×40 oil immersion lens with numerical aperture 1.3. The resulting fluorescence was recorded in a channel set up to detect emitted light in the range 510–600 nm. Islets were stimulated twice with 20 μM tolbutamide as described above. Images were collected at 2-s intervals, and fluorescence signals from individual cells were measured and analyzed as a function of time by using the Leica Confocal software package (Leica Microsystems). Results were plotted as the change in fluorescence intensity in arbitrary units. The images were analyzed using Leica confocal software.

In Paper V, after the detection of MitoTracker staining (see below) calcium responses from isolated ß-cells and from cells within intact islets were measured. Cross-talk from the green into the red channel was calculated in cells loaded with Fluo-3 only and was corrected for in subsequent experiments. Cells and islets were pre-perifused during 5 min and then stimulated with 20 mM glucose during 10 minutes. The resulting fluorescence was recorded in a channel set up to detect emitted green light in the range 510–560 nm. The Fluo-3 response in islets was recorded from one randomly chosen cross-section. The lag-time for Ca^{2+} rise was defined as the time from addition of stimulus until the onset of fluorescence rise and the magnitude was calculated as the change in fluorescence intensity (ΔF) expressed as a percentage of the basal fluorescence intensity (F0). The magnitude of calcium response was not

analyzed in islets because of difficulties in the precise alignment of cells during the measurement (Paper V).

Measurement of NAD(P)H fluorescence

Cells were incubated 40 min at 3 mM glucose without Fura-2 and then placed on the stage of a Nikon Diaphot-TMD (Japan) microscope system. Cells were excited at 340 nm during 125 ms. The resulting NAD(P)H autofluorescence was measured with a photomultiplier at 510 nm and expressed as arbitrary units. The interval between measurements was 1.26 s. ß-Cells were stimulated twice with 20 mM glucose or 20 mM KIC during 10 minutes with a resting period of 30 min at 3 mM glucose between the stimulations. Because measurement of NAD(P)H autofluorescence requires more intensive UV light than Fura-2 measurement, the registration period was limited to 4 minutes to reduce the risk of cell damage.

Experiment design and definition of response parameters

ß-Cells or islets were initially pre-perifused at 3 mM glucose for 15 min. Each ß-cell was then stimulated twice over 10-min periods with a resting period of 30 min between the stimulations, except for experiments from Paper V. The duration of stimulation and resting period were chosen to reduce the risk for persisting effects which may influence the second response (Nesher *et al* 1989) but with sufficient time to record individual profiles also from cells that respond late. All test media contained 3 mM glucose except in studies with 20 μM tolbutamide, which was applied in KRH medium containing 5 mM glucose to increase the amount of responding cells (Jonkers *et al* 2001). The two stimulation periods from the each cell were compared with regard to the timing and magnitude of changes in $[Ca^{2+}]_i$. The lag-time for the initial lowering was defined as the time from addition of stimulus until the first value below the baseline average, calculated during the 3 minutes preceding the stimulation. The depth of initial lowering (nadir) was calculated as the difference between the baseline and the lowest $[Ca^{2+}]_i$ value. The lag-time for the Ca^{2+} rise, was defined as the time from the addition of stimulus to the first $[Ca^{2+}]_i$ value above the extrapolated baseline in a continuing rise to a $[Ca^{2+}]_i$ peak (Fig 2). The magnitude of first $[Ca^{2+}]_i$ spike, i.e. peak height was calculated as the difference between the baseline and the highest $[Ca^{2+}]_i$ value during the first peak (Fig. 2). Superimposed spikes on top of the peaks were not included in those measurements. The experiments were not designed to study calcium oscillations.

   In Paper V, ß-cells were first scanned for MitoTracker staining, and their calcium response was then recorded during 10-min stimulation with 20 mM glucose.

Measurement of insulin release from intact islets

Isolated mouse islets were cultured overnight and loaded with Fura-2 during 40 minutes before being placed in a perifusion chamber (25-30 islets) enclosed in an incubator maintained at 37˚C (Larsson-Nyrén and Sehlin 1996). After 15-min preperifusion in KRH with 3 mM glucose, two consecutive glucose stimulations were performed with 20 mM glucose during 7 min with a 30 min period at 3 mM glucose

between the stimulations. Effluent fractions were collected over 15 s and 30 s intervals. Insulin was measured by RIA with mouse insulin as the standard (Heding 1966).

Measurement of insulin release from single ß-cells.

Zn^{2+} efflux was measured as a marker of insulin secretion, which is co-released with insulin (Fredrickson and Bush 2001). ß-Cells were prepared as described above. Zn^{2+} images with FluoZin-3 were acquired with 488 nm excitation and 510 nm emission using the Openlab image analysis system on the Zeiss Axiovert microscope (see *Measurements of cytoplasmic Ca^{2+} in ß-cells*)**.** Buffer with a reduced background Zn^{2+} level was prepared as described by Qian *et al* (2003). Briefly, KRH was prepared with all ingredients except calcium and magnesium salts. The buffer was then treated with 5g/dl Chelex-100 (Bio-Rad) for 2 h. The pH was adjusted to 7.4 after Chelex treatment and puratronic grade $CaCl_2$ and $MgSO_4$ were added to the final concentrations. During all experiments and solution preparation, glass containers were avoided to minimize metal contamination. The Zn^{2+} chelator 200 nM TPEN was added. Glass slides for cell preparation were soaked in 2 mM EDTA for 2-4 days to minimize Zn^{2+} leaching during the experiments (Kay 2004). Cover glasses with Fura-2 loaded cells were washed in 3 ml KRH containing 2μM FluoZin-3, placed as the bottom of the open chamber and transferred to the microscope. 150 μl KRH with Fluozin-3 was added to the chamber. To stimulate cells, 10 μl of tolbutamide stock solution containing 2μM FluoZin-3 was added to give a final concentration of 100 μM tolbutamide. Our preliminary experiments have shown that the final homogeneous concentration of the stimulator in the chamber is reached within about 5s. For controls, KRH buffer without tolbutamide was applied to the cells. FluoZin-3 fluorescence images were collected every 2s and the average fluorescence intensities were measured in a region of interest (ROI) of ~20 μm around the cell periphery. Cells were identified by DIC images before the measurement and by the low Zn-Fluozin background from the cell membrane. FluoZin-3 has undetectable penetration into the cell, presumably because of the three negative charges on the molecule at physiological pH (Gee *et al* 2002, Qian *et al* 2003). Cells were stimulated during 10 min, after which they were perifused with KRH containing 3 mM glucose for 30 min. After that, cells were again stimulated with 100 μM tolbutamide added to the perifusion medium and $[Ca^{2+}]_i$ was measured as described above. Attempts were not made to measure Zn^{2+} efflux and Ca^{2+} response simultaneously. Zn^{2+} measurements required higher excitation intensity than calcium measurements with Fura-2. The wavelengths used for calcium measurements (380 and 340 nm) can be harmful for cells during intense exposure. Our system does not allow a change of excitation exposure during simultaneous measurements. We have not compared the magnitudes of Zn^{2+} and Ca^{2+} response because Zn^{2+} dissolves quickly in the surrounding medium and the rise in Zn^{2+} outflow is difficult to estimate precisely.

Measurement of MitoTracker intensity

Experiments were performed using the Leica SP2 spectral laser scanning confocal microscopy system (Leica Microsystems, Mannheim, Germany). Glasses with cells labeled with Fluo-3 and MitoTracker Red were mounted as the bottom of an open perifusion chamber on the microscope stage and maintained at 37°C. Intact islets were

placed on coverslips on the bottom of the chamber. In islets, cells were first visualized using transmission laser scanning microscopy. Cells and islets were continuously superfused at a flow rate of 0.6 ml/min and imaged using Leica oil immersion objective lens (×63, zoom 4, for cells and ×40 for islets) with numerical aperture 1.3. The pinhole was adjusted to match the size of one airy unit for each objective and wavelength by the "Airy 1" function of the software. For z-series, the thickness of optical section was 0.6 μm. The pinhole was larger for calcium measurements in isolated ß-cells and islets to obtain the thickness of optical section μm. Images of red emission were acquired using excitation wavelength of 543 nm and a 590 nm long pass filter. z-Series scans of about 30 optical sections were made through each cell with 0.5 μm between layers. A maximum intensity projection of the confocal z-series of images of fluorescent images was created. Leica Confocal Software was used to quantify MitoTracker intensity in composite images, which allowed calculation of mean and S.D. of pixel intensities and the construction of three-dimensional and cross sectional profiles. The stained area in single cells was also measured in 3-D projection using a local threshold function and calculated as the proportion of the cell area taken by projected mitochondria. Based on calculation of the area of mitochondria in single sections, we found that a projected area of 60-70% corresponds to 3-4.5% of cell volume. To study the spatial relation between mitochondria and localised increases in $[Ca^{2+}]_i$, the calcium response was compared in areas (regions of interest, ROI) intensively stained with MitoTracker and in not stained and poorly stained areas.

Chemicals

Collagenase type I, HEPES and poly-L-lysine were purchased from Boehringer (Mannheim, Germany). BSA, fraction V. EGTA, L-glutamine, KIC, arginine and DNAase were all from Sigma Chemical Co. (St Louis, MO, U.S.A). Culture medium RPMI 1640 was obtained from ICN Biochemicals, and fetal calf serum was from Labkemi AB (Stockholm, Sweden). Fura 2-AM, Fluo-3, FluoZin-3, tetrakis (2-pyridylmethyl)ethilenediamine (TPEN) and Mitotracker Red CXMRos were from Molecular probes Inc. (Eugene, Oregon, USA). Puratronic $CaCl_2$ and $MgSO_4$ were from Alfa Aesar (Karlsruhe, Germany). Benzylpenicillin and garamycin were from Schering Co (Kenilworth, NJ, U.S.A). Glyceraldehyde was purchased from The British Drug Houses Ltd, United Kingdom, tolbutamide was from Hoechst AG, Germany. All other reagents were of analytical grade.

Statistical analysis

The data are presented as means ± S.E.M. Statistical significance for comparison of responses from the same cell or islet during first and second stimulation was evaluated using Student's t-test for paired data or the Mann–Whitney U-test. For comparison between sets of experiments two-tailed Student's t-test for unpaired data was used. Correlation coefficients (r) were computed by using Statworks software (Computer Associates International Islandia, N.Y., USA) or Microsoft Excel. The significance level was set at *p* less than 0.05. NS (non-significant) means P>0.05.

RESULTS

Glucose-induced Ca^{2+} response in single dispersed ß-cells

ob/ob Mouse (Paper I, II and III)

Parameters of Ca^{2+} response in Paper I were calculated in a different way than in papers II and III and are therefore presented in the text. Data from Papers II and III are shown in Table 1.

<u>Comparison of lag-times.</u> In Paper I the lag-time for [Ca^{2+}]$_i$ rise was defined as the time from addition of stimulus until the onset of increase. Lag-time for initial lowering was not calculated. The two stimulation periods from each cell were compared with regard to timing and magnitude of changes in [Ca^{2+}]$_i$. There was a correlation between lag-times for [Ca^{2+}]$_i$ rise with both 10 and 20 mM glucose. The correlation coefficient r was 0.94 for 10 mM glucose, P<0.001, with the averages 169±17 and 201±21 s (P<0.001), for 1st and 2nd stimulation, respectively. For 20 mM glucose the correlation coefficient r was 0.96 (P<0.001), with the averages 170±18 and 183±20 s (P<0.025). Most of the cells reacted with a [Ca^{2+}]$_i$ rise within 3 min from the start of stimulation. However, some ß-cells did not respond with a [Ca^{2+}]$_i$ rise until 7 - 9 min after stimulation. The lag-time during the second stimulation was longer than during the first one both in fast and late responding cells (19% at 10 mM glucose and 8% at 20 mM glucose). The response pattern, including nadir of initial lowering and peak height, was similar in cells with short and long lag-time, i.e. the duration of the lag-time had little influence on the response pattern. Table 1 shows lag-times for [Ca^{2+}]$_i$ rise and initial lowering in *ob/ob* mouse ß-cells combined from Papers II and III. The pattern of cell specificity of ß-cell response was the same as in Paper I.

<u>Comparison of initial lowering nadirs, peak heights and response patterns</u>. Nadirs of initial lowering showed a correlation coefficient with 10 and 20 mM glucose. The correlation coefficient for nadirs of initial lowering was r=0.93, P=0.001 for ß-cells exposed twice to 10 mM glucose (51±3 and 64±4 nM, 1st and 2nd stimulation, respectively; P<0.05) and r=0.79, P<0.001 for ß-cells exposed twice to 20 mM glucose (48±2 and 63±2 nM, 1st and 2nd stimulation, respectively; P<0.005). The peak height in Paper I was calculated as the highest [Ca^{2+}]$_i$ value during the first peak. The correlation coefficient for peak heights was r=0.51, P<0.01 (average 719±32 and 716±31 nM, 1st and 2nd stimulation) with 10 mM glucose. With 20 mM glucose the correlation coefficient was r=0.77, P<0.001 (average 743±25 and 747±27 nM, 1st and 2nd stimulation, respectively). Peak heights of *ob/ob* mouse ß-cell responses from Paper II and III and their correlation

coefficients are shown in Table 1. In the majority of individual ß-cells the pattern of first response was very similar to the second one (Figure 3 in Paper I).

Lean mouse and rat (Paper II)

The lag-times for $[Ca^{2+}]_i$ rise in lean mouse ß-cells and rat ß-cells were similar to those obtained in single *ob/ob* mouse ß-cells, and there was a significant correlation between the lag-times (Table 1). Ca^{2+} response parameters in glucose-stimulated lean mouse ß-cells from Papers II and III are presented in Table 1. The lag-time for initial lowering was shorter in ß-cells from lean mice and rats than in *ob/ob* mouse ß-cells, P<0.01 when comparing 78 s with 47 s (lean mouse) or 48 s (rat). There was a correlation between lag-times for initial lowering in lean mouse ß-cells (Table 1). The correlation for the nadir of initial $[Ca^{2+}]_i$ lowering was r=0.1, NS (32±3 and 26±2 nM Ca^{2+}, first and second stimulation, NS). Corresponding values in rat ß-cells were r=0.57, P<0.01 (39 ±4 and 40 ±4 nM Ca^{2+}, NS). The magnitude of the calcium rise was nearly the same in single dispersed ß-cells from lean mice and rats as in single dispersed *ob/ob* ß-cells, with a significant correlation within the pairs of stimulation in all three types of ß-cells (Table 1).

db/db Mouse (Paper III)

Lag-times for calcium rise in were longer *db/db* mouse ß-cells than in lean mouse ß-cells but showed a correlation between stimulations (Table 1). Seventeen out of 30 (17/30) ß-cells showed initial lowering during both stimulations, which was fewer than in lean mouse ß-cells (21/23) (p<0.001, using Chi-square test with Yates' correction). Lag-times for initial lowering were cell-specific (Table 1). Nadirs of initial lowering were not correlated (r=0.26, NS) and showed no difference between the stimulations (50±16 and 30±7 nM Ca^{2+}, first and second stimulation, respectively, NS). Although the magnitude of calcium response was lower than in lean mouse ß-cells, peak heights were cell-specific (Table 1). Basal $[Ca^{2+}]_i$ levels were higher than in lean and *ob/ob* mouse ß-cells (130±15 nM vs. 56±3 nM and 93±12 nM Ca^{2+}).

We compared timing and magnitude of responses with (17/30) and without initial lowering (13/30). Lag-times did not differ between the groups (189±36 s and 215±36 s, respectively, NS, first stimulation; 152±30 s and 198±33 s, respectively, NS, second stimulation). Responses with initial lowering had higher magnitude. This was observed both during the first (100±25 nM and 221±35 nM Ca2+, P<0.01) and the second stimulation (134±14 nM and 241±44 nM Ca2+, P<0.01). Timing and magnitude of response were cell-specific in both groups.

Glucose-induced Ca^{2+} response in ß-cell clusters and islets (Paper II)

Three cluster models were used. First, calcium response was investigated in one single ß-cell within a small cluster from *ob/ob* mouse, referred as 'single ß-cell

within a small cluster'. The cluster consisted of three or four cells in physical contact. Then we enlarged the measurement area and studied temporal Ca^{2+} profiles in whole medium (about 10 cells) and large size clusters (about 25 cells).

Comparison of lag-times. Lag-times for $[Ca^{2+}]_i$ rise and for initial $[Ca^{2+}]_i$ lowering were cell-specific in 'single ß-cell within a small cluster' (Table 1). Responses from the majority of medium size clusters were very similar to those obtained from big clusters. There was a strong correlation between the first and second lag-time for $[Ca^{2+}]_i$ rise in both sets of experiments. Lag-times for initial lowering showed a correlation only in medium size clusters. In large clusters, lag-time for $[Ca^{2+}]_i$ rise was shorter (<1min) than in single dispersed ß-cells and 'single ß-cells within a small cluster' (Table 1).

Intact islets showed longer lag-times for $[Ca^{2+}]_i$ rise when compared with medium and large size clusters. Lag-times for $[Ca^{2+}]_i$ rise were cell-specific in islets from *ob/ob* but not from lean mice. Lean mouse islets responded with a longer lag-time during the first stimulation, and *ob/ob* mouse islets responded with a longer lag-time during the second stimulation (Table 1).

Comparison of nadirs of initial lowering and peak heights. 'Single ß-cells within a small cluster' showed cell-specific nadirs of initial lowering in $[Ca^{2+}]_i$ (24±2 and 29±2 nM Ca^{2+}, P<0.05 with r=0.59, P<0.001). Initial lowerings were observed during both stimulations in 4/19 medium size clusters (9 ±3 and 10 ±2 nM Ca2+, r=0.68) and in 4/22 large clusters (21±9 and 24 ±9 nM Ca2+, r=0.49). For lean mouse islets the corresponding values were 10±1 and 4±1 nM Ca2 + (P<0.001), with a correlation of r=0.59 (P<0.05). Lag-times for initial lowering were not cell-specific in lean mouse islets. Initial lowerings were seldom observed in islets from *ob/ob* mice. Peak heights were cell-specific in cluster models and intact islets. The peak heights were reduced as the number of cells in contact increased (Table 1). The first peak height was lower than the second one in clusters and in lean and *ob/ob* mouse islets (Table 1).

Insulin release dynamics in ob/ob mouse islets (Paper II)

We measured insulin release from perifused *ob/ob* mouse islets to determine if the prolonged lag-time and reduced Ca^{2+} response observed during the second glucose stimulation corresponded to the time of onset and amount of insulin release, (Fig. 4C and 4D in Paper II). Batches of 25-30 islets were stimulated twice with 20 mM glucose following the same protocol as for the $[Ca^{2+}]_i$ measurements. Onset of stimulated secretion was delayed (from 45–60 s to 60–75 s) during the second exposure to 20 mM glucose (P<0.05, using the Mann–Whitney U-test). The total amount of secretion was lower during the second stimulation (0.027±0.005 ng/islet/min and 0.011±0.003 ng/islet/min, first and second stimulation, respectively, P<0.001).

Ca^{2+} response to nutrient and non-nutrient insulin secretagogues in lean, *ob/ob* and *db/db* mouse ß-cells (Paper III and IV)

Glyceraldehyde

When single dispersed lean, *ob/ob* and *db/db* mouse ß-cells were stimulated with the glycolytic intermediate, 10 mM glyceraldehyde, the Ca^{2+} pattern was similar to glucose-induced Ca^{2+} changes. Lag-times for calcium rise and peak heights were cell-specific in all three animal models (Table 1 and 3).

In lean mouse ß-cells, lag-times for initial lowering were cell-specific and nadirs of initial lowering also showed a correlation (r=0.62, P<0.001; 18±5 and 20±3 nM Ca^{2+}, first and second stimulation, NS). Peak height was smaller during the second stimulation, but peak heights showed a correlation between the first and second stimulation (Table 1).

In *ob/ob* mouse ß-cells, the response patterns were almost identical during the first and second exposure, but the lag-time for initial lowering in *ob/ob* mouse ß-cells showed no correlation within the pairs (Table 1). Nadirs of initial lowering were the same during both stimulations (27±4 and 25±3 nM Ca^{2+}, first and second stimulation, respectively, NS) and showed a correlation of r=0.69 (P<0.001).

In *db/db* mouse ß-cells, initial [Ca^{2+}]$_i$ lowerings were observed in only 2 out of 13 cells (2/13). Peak heights were lower compared with glyceraldehyde-induced responses from lean mouse ß-cells, but there was no difference in lag-time for calcium rise (Table 1).

KIC

The mitochondrial substrate, 20 mM KIC, induced cell-specific responses both with regard to timing and magnitude in ß-cells from lean but not from *ob/ob* or *db/db* mice (Table 1 and 3). The [Ca^{2+}]$_i$ rise occurred earlier than when glucose or glyceraldehyde was applied (Table 1, P<0.001). Initial lowering less pronounced (Lenzen *et al* 2000) and was observed during both stimulations in 6/16 cells. This is in line with previous observations. There was no correlation between lag-times for initial lowering (Table 1) or between nadirs (r=-0.96, NS).

ob/ob Mouse ß-cells showed a correlation between peak heights (Table 1). Initial lowerings were observed in 25/31 cells during both stimulations. There was no correlation of lag-times for initial lowering (Table 1) or the nadirs (20±3 and 26±3 nM Ca^{2+}, r=-0.14, NS). The rise during the second stimulation occurred with a shorter lag-time than during the first stimulation (Table 1) and had a smaller variation (0-390 s vs.0-155 s).

In *db/db* mouse ß-cells, peak heights were also cell-specific (Table 1). As in *ob/ob* mouse ß-cells, the second lag-time was shorter and varied less than the first (75-346 s vs. 68-208 s). Initial lowering was observed during both stimulations in

only 2/14 cells. The Ca^{2+} response to KIC was delayed and reduced when compared with lean mouse ß-cells (Table 1, $p<0.05$).

Tolbutamide and arginine

When the K_{ATP}-channel blocker, 100 µM tolbutamide was applied, the lag-time and magnitude of $[Ca^{2+}]_i$ rise were cell-specific in lean mouse ß-cells but not in *ob/ob* or *db/db* mouse ß-cells (Table 1). Unlike glucose, tolbutamide induced responses with a shorter lag-time in ß-cells from hyperglycemic mice when compared with lean mouse ß-cells. There was no initial lowering of $[Ca^{2+}]_i$ before the rise, probably because initial lowering is regulated by metabolism (Lund *et al* 1989). In *ob/ob* mouse ß-cells, the peak height was lower during the second stimulation than during the first one (Table 1). We then tested tolbutamide at 20 µM to find out if the lag-time is concentration-dependent. The lower concentration could provide more heterogeneous responses with regard to timing and reduce the risk for persisting effects after the first stimulation. As with 100 µM tolbutamide, the timing of response was cell-specific only in lean mouse ß-cells. Peak heights were cell-specific in all three models (Table 1). The lag-time for $[Ca^{2+}]_i$ rise was longer than in experiments with 100 µM tolbutamide (Table 1, $P<0.01$).

Arginine induced cell-specific Ca^{2+} responses in lean mouse ß-cells (Table 1). There was no correlation between lag-times for calcium rise during the first and second stimulation in ß-cells from *db/db* or *ob/ob* mice, but peak heights were cell-specific in *db/db* mouse ß-cells (Table1). As with tolbutamide, the response in *db/db* mouse ß-cells occurred with shorter lag-times than in lean mouse ß-cells and reached a lower magnitude.

Thus, ß-cell ion channel function seems to be cell-specific in normal mice but not in hyperglycemic mice (Table 3).

Table 1. Comparison of lag-times for initial lowering, lag-times for $[Ca^{2+}]_i$ rise and peak heights of $[Ca^{2+}]_i$ responses during two consecutive stimulations. Data is presented as mean values±S.E.M. for the number of experiments given in parenthesis. Data for glucose-stimulated lean and *ob/ob* mouse ß-cells are combined from papers II and III. Degree of significance for difference within the pairs and correlation coefficient was determined by two-tailed, paired Student's *t*-test. *P<0.05, **P<0.005, ***P<0.001, when testing significance of correlation between first and second stimulation. [a]P<0.05, [aa]P<0.005, [aaa]P<0.001, when comparing response parameters between first and second stimulation. [b]P<0.05, [bb]P<0.005, [bbb]P<0.001, when comparing *db/db* and lean mouse ß-cells, [c]P<0.05, [cc]P<0.005, [ccc]P<0.001, when comparing *ob/ob* and lean mouse ß-cells.

Table.1

|	Lag-time for initial lowering (s)			Lag-time for calcium rise (s)			Peak height (nM Ca^{2+})		
	1 stim	2 stim	r	1 stim	2 stim	r	1 stim	2 stim	r
20 mM glucose									
lean mouse ß-cells (48)	47±8	62±10[*] (n=43)	0.85[***]	137±9 [b]	157±13[a] [b]	0.67[***]	486±23 [bbb]	475±31 [bbb]	0.75[***]
db/db mouse ß-cells (30)	42±11	57±10 (n=17)	0.71[**]	224±26	211±21	0.74[**]	180±26	205±30	0.50[**]
ob/ob mouse ß-cells (38)	68±8	102±14[*] (n=32)	0.91[***]	157±14	192±16[aaa]	0.87[***]	532±39	497±37	0.77[***]
rat ß-cells (39)	48±8	43±9 (n=22)	0.38[NS]	125±10	122±16	0.77[***]	564±42	615±66	0.48[***]
single ß-cells within a small cluster (53)	37±5	39±5 (n=47)	0.57[***]	121±11	150±14[aaa]	0.89[***]	662±27	655±22	0.64[***]
medium size clusters (19)	13±5	13±6 (n=4)	0.72[NS]	38±4	44±4	0.73[***]	400±19	324±17	0.82[***]
large size clusters (22)	14±4	22±6 (n=4)	0.99[***]	29±3	33±7	0.45[*]	345±18	240±16	0.94[***]
ob/ob mouse islets (27)	-	-	-	51 ±3	71 ±6[aa]	0.43[*]	147±17	65±8[aaa]	0.60[***]
lean mouse islets (17)	41±4	36±3 (n=12)	0.31[NS]	87±6	65±3[a]	0.35[NS]	178±11	142±9	0.89[***]
10 mM glyceraldehyde									
lean mouse ß-cells (13)	35±4	48±8 (n=10)	0.69[**]	113±23 [b]	161±24 [b]	0.76[**]	274±27 [bbb]	219±29[a] [bbb]	0.89[**]
db/db mouse ß-cells (13)	57±50	94±37 (n=2)	-	151±35	174±32	0.91[**]	160±25	125±24	0.74[***]
ob/ob mouse ß-cells (17)	25±9	51±16 (n=11)	0.40[NS]	143±19	159±20	0.75[***]	447±56	450±75	0.71[**]
20 mM KIC									
lean mouse ß-cells (16)	21±8	36±11 (n=6)	0.23 NS	68±10	75±11	0.84**	235±31	270±37	0.59**
db/db mouse ß-cells (14)	106±34	94±36	-0.04 NS	191±18	116±15[b]	0.43 NS	119±17	136±23	0.85***
ob/ob mouse ß-cells (31)	29±9	29±6 (n=25)	-0.04[NS]	107±18	67±7[*]	-0.01[NS]	250±24	279±24	0.60[***]
100 μM tolbutamide									
lean mouse ß-cells (20)	-	-	-	85±10 [b]	84±15	0.74[***]	392±49 [bbb]	360±43 [bbb]	0.52[*]
db/db mouse ß-cells (11)	-	-	-	52±9	76±21	0.31[NS]	112±14	146±20	0.37[NS]
ob/ob mouse ß-cells (24)	-	-	-	45±14	70±24[a]	0.10[NS]	478±54	325±32[**]	0.36[NS]
100 μM tolbutamide, insulin and Ca^{2+} response, see explanation in Results, p. 27									
lean mouse ß-cells (16)	-	-	-	101±28	113±23	0.68*	-	-	
ob/ob mouse ß-cells (10)	-	-	-	68±9	75±18	0.14[NS]	-	-	
20 μM tolbutamide									
lean mouse ß-cells (15)	-	-	-	193±32 [b]	245±37 [b]	0.74**	422±71 [bbb]	343±61 [bbb]	0.85[***]
db/db mouse ß-cells (11)	-	-	-	103±28	101±24	-0.08[NS]	105±35	133±39	0.71[*]
ob/ob mouse ß-cells (13)	-	-	-	163±45	185±35	0.24[NS]	416±69	325±49[aa]	0.84[***]
ß-cells in lean mouse islets (30)	-	-	-	46±7 [c]	43±6 [c]	0.65[***]	30±4	17±2[aa]	0.47[**]
ß-cells in *ob/ob* mouse islets (86)	-	-	-	123±9	198±14[aaa]	0.39[***]	28±4	21±2	-0.08[NS]
10 mM arginine									
lean mouse ß-cells (13)	-	-	-	170±30 [bb]	181±30	0.72[**]	213±32 [bbb]	167±19 [bbb]	0.63[*]
db/db mouse ß-cells (11)	-	-	-	89±19	142±27	-0.29[NS]	111±20	54±14[aa]	0.78[**]
ob/ob mouse ß-cells (13)	-	-	-	156±37	163±36	0.20[NS]	158±24	156±21	0.49[NS]
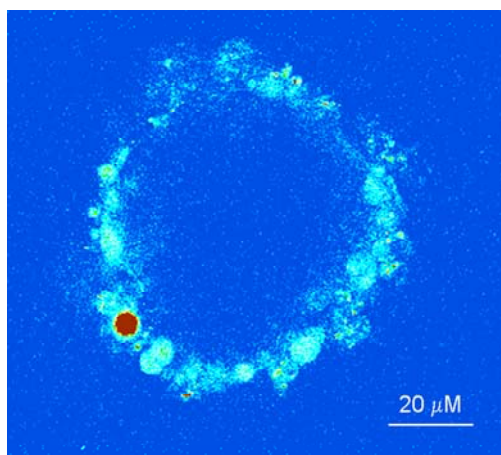
Figure 3. An image of an islet of Langerhans loaded with Fluo-3 and stimulated with 20 μM tolbutamide + 5mM glucose.

Cell specificity of Ca^{2+} response to tolbutamide in single ß-cells within intact islets

We studied responses from individual ß-cells on the periphery of Fluo-3-labeled intact islets (Fig. 3) during two consecutive stimulations with 20 μM tolbutamide We tested 30 cells in 6 lean mouse islets and 87 cells in 10 *ob/ob* mouse islets. ß-Cells within lean mouse islets showed cell-specific responses with a high degree of correlation between lag-times during the first and second stimulation (Fig. 4C in Paper IV). Within each islet, there was only a small variation in lag-time between different cells and between the first and second stimulation (Table 1). Peak heights were cell-specific (Table 1).

ß-Cells within *ob/ob* mouse islets also showed cell-specific timing of responses (Table 1). The average lag-time was longer than in lean mouse (Table 1) and varied more between individual cells (in 0-350 *ob/ob* mouse islets vs. 0-128 in lean mouse islets). Thus, individual ß-cells within an *ob/ob* mouse islet showed temporal cell specificity of the Ca^{2+} response.

NAD(P)H response to glucose and KIC in individual lean, *ob/ob* and *db/db* mouse ß-cells (Paper III)

Similar to what we found for Ca^{2+} responses, 20 mM glucose induced cell-specific NAD(P)H responses with regard to timing and magnitude in all three animal models (Table 2). Timing and magnitude of NAD(P)H rise to 20 mM KIC were cell-specific in lean mouse ß-cells but not in *db/db* mouse ß-cells (Table 2). ß-Cells from *ob/ob* mice showed no cell specific timing of the response, but the fluorescence increases showed a correlation between the first and second stimulation.

Table 2. Glucose- and KIC-induced NAD(P)H response in ß-cells. Data is presented as mean values±S.E.M. for the number of experiments given in parenthesis. *P<0.05, **P<0.005, ***P<0.001.

	Lag-time 1 (s)	Lag-time 2 (s)	r	Fluorescence increase 1 (a.u.)	Fluorescence increase 2 (a.u.)	r
20 mM glucose						
lean mouse ß-cells (11)	38±6	40±5	0.60**	10±2	10±1	0.56*
db/db mouse ß-cells (13)	46±11	46±10	0.54*	7±1	7±1	0.85**
ob/ob mouse ß-cells (17)	41±9	48±7	0.80**	11±2	9±1	0.70**
20 mM KIC						
lean mouse ß-cells (14)	27±3	24±4	0.55*	7±1	4±1	0.72**
db/db mouse ß-cells (11)	49±8	32±4	0.39[NS]	6±1	6±1	0.40[NS]
ob/ob mouse ß-cells (15)	32±6	33±7	0.46[NS]	7±1	5±1	0.56*

Insulin secretion in isolated ß-cells from lean and *ob/ob* mice (Paper IV)

We have also tested to what extent temporal cell specificity of the calcium response is related to insulin release. Zn^{2+} is co-released with insulin and Zn^{2+} efflux was measured as a marker of insulin secretion (Qian *et al* 2003). The secretory response to 100 µM tolbutamide was recorded during the first stimulation and the Ca^{2+} response was recorded during the second stimulation (Fig. 3 in Paper IV). We found that the time of onset of Zn^{2+} outflow correlated with the lag-time for calcium rise in lean mouse ß-cells but not in *ob/ob* mouse ß-cells (Table 1).

Table 3. Temporal cell specificity of ß-cell stimulus-secretion coupling in studied models.

Model	Glycolysis	Mitochondrial metabolism	Ion channels
Normal ß-cells	+	+	+
Hyperglycemic mouse ß-cells (*ob/ob* and *db/db*)	+	-	-

Mitochondrial state and Ca^{2+} response in ß-cells (Paper V)

The morphology of mitochondria ranged from small grains to large elongated or spindle-shaped structures (Fig. 4A and 4B). Mitochondria were observed mostly around the nucleus, they were unevenly distributed, and many of them seemed to be connected. To compare the mitochondrial mass between lean (N=9) and obese mice (N=22), we analyzed the MitoTracker staining intensity and the area taken by mitochondria projected onto the cell middle section. The projected area percentage was higher in lean mouse ß-cells than in *ob/ob* mouse ß-cells (72±5 % and 50±4 %, respectively, P<0.05) but the intensity of MitoTracker staining did not differ (137±14 a.u. and 116±8 a.u., respectively, NS). The intensity showed a correlation with the stained area both in lean and obese mouse ß-cells (r=0.85, P<0.01 and r=0.42, P<0.05).
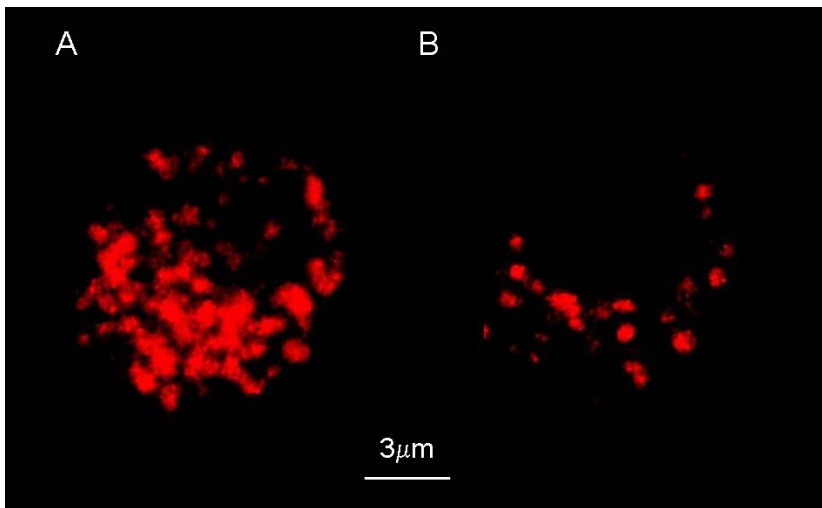

Figure 4. Active mitochondria in a single lean mouse ß-cell stained with MitoTracker Red CMXRos and examined by fluorescence microscopy. Panel A shows a projection of a z-series comprising 24 slices acquired at 0.5 μm intervals. Panel B shows one section from the series.

The intensity of Mitotracker staining in ß-cells before the stimulation was analyzed together with the lag-times and magnitude of the calcium response to 20 mM glucose. The mitochondrial mass was inversely correlated with the lag-times for $[Ca^{2+}]_i$ rise in both lean and *ob/ob* mouse ß-cells (r=-0.73 and r=-0.43, respectively, P<0.05). Thus, cells with short lag-times had a higher amount of active mitochondria before the stimulation. The Fluo-3 increase was lower in ß-cells from lean mice than in *ob/ob* mouse ß-cells (42±9 % and 85±12 %, P<0.001).

There was no correlation between the magnitude of responses and the mitochondrial mass in either lean or *ob/ob* mouse ß-cells (r=0.15 and r=0.05, NS).

The $[Ca^{2+}]_i$ rise occurs as localized $[Ca^{2+}]_i$ increases within the ß-cell (Bokvist *et al* 1995, Qian and Kennedy 2001). We investigated whether areas of those increases were co-located with mitochondria. Fluo-3 does not enter organelles and therefore we assume that only cytoplasmic free calcium was measured. Responses in different areas of the ß-cell cytoplasm were almost simultaneous with the time-scale used but varied in magnitude. Traces with a steep rise and a high magnitude suggested "hot spots" of intracellular calcium dynamics. In some cytoplasmic areas no $[Ca^{2+}]_i$ increase was observed (Fig. 3A and 3C in Paper V). We tested the correlation between the MitoTracker intensity and the Fluo-3 fluorescence increases in different ROIs. We found an inverse correlation between the magnitude of $[Ca^{2+}]_i$ rise and the MitoTracker intensity (r=-0.64, P<0.001). It seemed logical, since mitochondria were observed mostly around the nucleus, and the calcium channels are situated on the membrane. We then compared the magnitude of response in ROIs along the membrane near areas densely populated with mitochondria (group 1) and on the opposite side of the cell, where fewer mitochondria were observed (group 2). The magnitude of calcium increases was not correlated with the proximity of active mitochondria (95±29% and 55±13%, group 1 and group 2, respectively, N=9 lean mouse ß-cells, NS).

To find out if it is possible to use MitoTracker fluorescence intensity to identify fast-reacting cells within intact islets, we measured the mitochondrial mass in individual cells within islets from lean and *ob/ob* mice and subsequently registered their calcium response. We tested 26 cells in 3 lean mouse islets and 33 cells in 3 *ob/ob* mouse islets. There was a narrow range of lag-times for $[Ca^{2+}]_i$ rise between ß-cells within each lean mouse islet. Lag-times in ß-cells within *ob/ob* mouse islets showed a larger variation. In most islets, no correlation was found between the lag-times for $[Ca^{2+}]_i$ rise and the MitoTracker staining intensity. One of the *ob/ob* mouse islets showed r=-0.48 (P<0.05, N=18 cells).

DISCUSSION

Paper I reports on the early $[Ca^{2+}]_i$ dynamics elicited by consecutive glucose stimulations in *ob/ob* mouse ß-cells. The lag-time for $[Ca^{2+}]_i$ rise, the nadir of initial $[Ca^{2+}]_i$ lowering and the height of first peak showed a correlation within the pairs when the conditions during the two stimulations were not altered. The results therefore suggest that the response from single ß-cells have unique and reproducible characteristics. Heterogeneous Ca^{2+} handling has been observed also in airway epithelial cells (Evans and Sanderson 1999), HIT insulinoma cells (Prentki *et al* 1988), hepatocytes (Rooney *et al* 1989) and astrocytes (Yagodin *et al* 1995).

We analysed variations in lag-time for $[Ca^{2+}]_i$ rise between different ß-cells and between the two test periods for each ß-cell. It was found that at both 10 and 20 mM glucose the second lag period was slightly longer than the first (Paper I), which is interesting because the second stimulation also tended to cause a larger initial lowering in the Ca^{2+} level. However, because this enlarged lowering was only seen at 20 mM and not at 10 mM glucose and there was no correlation between the lag-times and initial dips in Ca^{2+} level at either 10 or 20 mM glucose, there seems to be no clear-cut relationship between these two glucose effects.

Some ß-cells showed a very late response to glucose. Different timing for $[Ca^{2+}]_i$ response could be an indication of various degrees of cell damage. It is also possible that damaged cells can show reproducible response patterns. However, cell damage is not likely to be the reason why the response is reproducible and is observed also in clusters of cells and in intact islets (Paper II). It is quite remarkable that the response pattern was similar in early and late-responding cells. This indicates that the lag-time and the pattern of $[Ca^{2+}]_i$ changes are controlled by different mechanisms.

ß-Cells from normoglycemic mice and rats also showed reproducible $[Ca^{2+}]_i$ changes (Paper II). Although mouse and rat pancreatic islets differ with regard to glucose-induced changes in cytoplasmic calcium (Antunes *et al* 2000), a cell-specific response at the single cell level was observed in both species. The lag-times for $[Ca^{2+}]_i$ rise were very similar in single dispersed ß-cells from both lean and *ob/ob* mice and from rat. However, the lag-time for initial lowering was nearly twice as long in *ob/ob* mouse ß-cells, when compared with ß-cells from lean mice and rat. This suggests that the metabolic signal(s) differ for onset of initial lowering and later $[Ca^{2+}]_i$ rise.

In Paper II we show that the timing of the Ca^{2+} response and the magnitude of response can be reproduced during a second stimulation both in ß-cells in clusters of different size and in intact islets. We also find that the lag-time for initial lowering and $[Ca^{2+}]_i$ rise is reduced when the number of cells in contact is increased. The shorter lag-time may depend on cell-to-cell transfer of signals. With the experimental set up it was not possible to study Ca^{2+} profiles from individual cells within either medium or large size clusters. We, therefore, cannot say how many fast reacting ß-cells (Paper I) need to be in contact to reduce the lag-times to the extent observed when comparing single ß-cells and medium size clusters. Jonkers *et al* (1999) have shown that the number of cells responding to a particular glucose concentration is enhanced in clusters of as few as 2–50 cells.

A delayed and reduced second $[Ca^{2+}]_i$ response in *ob/ob* islets corresponds to the findings on insulin secretion. A later response during the second stimulation conforms to previous finding of a stepwise reduction in insulin release dynamics in response to repeated glucose stimulations in perfused pancreata from C56BL/KsJ-mice (Berglund 1980). It may be that inhibitory signals produced during the first exposure are more effective when the cluster architecture is intact. Ionic events and diffusible compounds, such as NO (Grapengiesser *et al* 1999), may carry such inhibitory signals.

The strong reproducibility of the early $[Ca^{2+}]_i$ changes suggests that each ß-cell has a cell-specific capacity to respond to a glucose challenge within a certain time and with a unique response pattern. Individual ß-cells may have different roles in intact pancreatic islets. It has been suggested that there are subpopulations of ß-cells, which act as sensors within islets capable of initiating an appropriate response in other, less sensitive cells (Hiriart and Ramirez-Medeles 1991, Van Schravendijk *et al* 1992). The possibility that a subset of ß-cells have an actual pacemaker function has also been discussed (Cook 1984, Palti *et al* 1996, Aslanidi *et al* 2002) but the mechanisms underlying such a function are unclear. ß-Cells maintain their individual responses when they are functionally coupled in clusters and islets. This in line with the study by Jonkers *et al* (1999) suggesting the possibility that that the fastest cells in an islet entrains all the other ß-cells, to which it is electrically coupled. However, intercellular coupling or paracrine influences *in vivo* may also erase individual differences of ß-cells and create a functionally more homogenous population.

An important question was whether cell specificity of ß-cell response is impaired in hyperglycemia and type 2 diabetes (Paper III). We found that *db/db* mouse ß-cells show cell-specific responses to glucose. Thus, cell specificity is not by itself a sign of normal ß-cell function. However, when several insulin secretagogues were tested, ß-cells from normal and hyperglycemic mice showed different patterns. Cells from lean mice showed cell-specific Ca^{2+} responses to all tested stimulators, which enter the stimulus-secretion coupling at different steps. This indicates that the response of each individual cell is under tight control and that the activity of several steps is cell-specific. Data on NAD(P)H responses to glucose and KIC suggest that cell specificity of nutrient-induced calcium response is determined by steps not later than mitochondrial metabolism. ß-Cells from *ob/ob* and *db/db* mice showed no cell-specific timing of NAD(P)H responses when stimulated with KIC. There was also no cell-specific lag-time for calcium rise in ß-cells from hyperglycemic mice with KIC, tolbutamide or arginine. Bypassing glycolysis or the whole metabolism caused a loss of temporal cell specificity in hyperglycemic mouse ß-cells but the magnitude of calcium response was still cell-specific. This allows us to make some further assumptions. Firstly, timing and magnitude of ß-cell response are controlled by different mechanisms. Secondly, mitochondrial function and ion channel function seem to be cell-specific in normal ß-cells but not in *db/db* and *ob/ob* mouse ß-cells. Glycolysis signals can generate a cell-specific response also when mitochondrial metabolism cannot. Thirdly, tests for cell specificity of ß-cell responses can be an important tool for studies of normal and disturbed ß-cell function.

ß-Cells from *db/db* mice showed delayed and reduced glucose-induced $[Ca^{2+}]_i$ responses and higher basal $[Ca^{2+}]_i$ levels, when compared with lean mouse ß-cells. This is similar to what has been shown earlier on insulin release and Ca^{2+} response for animals with hereditary and chemically induced type 2 diabetes (Berglund *et al* 1984, Roe *et al* 1994, Lindström *et al* 1996, Zaitsev *et al* 1997, Marie *et al* 2001). Mitochondrial dysfunction in type 2 diabetes has also been described (Maechler and Wollheim 2001, Malaisse 1993). The altered mitochondrial metabolism in *db/db* mouse ß-cells in experiments with KIC can be a sign of such dysfunction.

However, such changes were found also in *ob/ob* mice, whose ß-cells respond adequately to glucose stimulation (Hahn *et al* 1974, Hellman *et al* 1974) and where most aspects of mitochondrial metabolism are normal (Idahl and Lembert, 1995). Therefore the altered mitochondrial function could be a compensatory mechanism to prolonged hyperglycaemia.

Exogenously added glyceraldehyde enters the glycolytic pathway via its phosphorylation in the triokinase reaction to yield glyceraldehyde phosphate (MacDonald 1989). The subsequent metabolism is probably identical to that of glyceraldehyde phosphate derived from glucose. Glyceraldehyde can cause acidification of the ß-cell, which may affect the cell function (MacDonald 1989) The Ca^{2+} response to glyceraldehyde was cell-specific in lean, *ob/ob* and *db/db* mouse ß-cells, and the lag-time for calcium rise was the same with glyceraldehyde as with glucose. It is therefore possible that later parts of glycolysis are more important than the earliest metabolic steps including the glucokinase reaction for determining whether a cell reacts fast or slow. Lag-time for initial lowering was shorter in the presence of glyceraldehyde than in the presence of glucose. As already suggested above, various aspects of the Ca^{2+} response are probably controlled by different steps of the stimulus-secretion coupling, i.e. the lag-time for the lowering in Ca^{2+} may be controlled by early metabolic steps closer to the glucose phosphorylation, whereas lag-time for $[Ca^{2+}]_i$ rise is determined by later metabolic events. This may be why the lag-time for initial lowering was not reproduced during the second stimulation in studies with glyceraldehyde.

KIC is a transamination partner, which feeds into mitochondrial metabolism through α-ketoglutarate (Lembert and Idahl 1998) and induces a rapid increase in mitochondrial NADH generation (Panten 1975). KIC shortened the lag-time for calcium rise during the second stimulation in *ob/ob* and *db/db* mouse ß-cells but not in lean mouse ß-cells. The lag-times for the calcium rise in ß-cells from hyperglycemic mice showed a smaller variation during the second stimulation than during the first stimulation. Therefore, the difference between lag-times for calcium rise was more pronounced in cells responding late during the first stimulation. Precise mechanism of the accelerating effect of KIC on the calcium response in *ob/ob* and *db/db* mouse ß-cells remains to be clarified, but this observation suggests an intriguing possibility to specifically improve ß-cell function in diabetic animals.

Normal ß-cells had unique and reproducible, i.e. cell-specific, calcium responses also to the non-metabolic stimulators tolbutamide and arginine. This indicates cell specificity not only of the stimulus-secretion coupling, as a whole, but also of different parts of it. While cell specificity seems to be a robust phenomenon in normal ß-cells, *ob/ob* and *db/db* mouse ß-cells show no cell-specific timing of calcium response when stimulated with tolbutamide or arginine. The mechanism of action of arginine is a direct depolarisation of the ß-cell membrane similar to cations (Herchuelz *et al* 1984, Charles *et al* 1982). This means that the function of Ca^{2+} and maybe K^+_{ATP} channels is cell-specific in ß-cells from normal mice but not in *ob/ob* and *db/db* mouse ß-cells. Cell-specific function of calcium channels may be linked to the number of channels and/or differences in channel properties, such

as the gating. Previous reports have shown different results regarding calcium channel function in ß-cells from animals with conditions similar to type 2 diabetes. A reduction of L-type Ca^{2+} currents and a decreased expression of alpha 1-subunit of L-type Ca^{2+} channels was observed in the Zucker diabetic fatty rat (Roe *et al* 1996). Other studies report an increased activity of L-type Ca^{2+} channels in the GK rat (Kato *et al* 1996). A lower expression of Ca^{2+} channels can explain the reduced calcium response in type 2 diabetes but not the loss of temporal cell specificity, which we found in *db/db* and *ob/ob* mouse ß-cells. This indicates that other alterations of Ca^{2+} channels are present in ß-cells hyperglycemic mice (Kato *et al* 1996).

The failure of *db/db* and *ob/ob* mouse ß-cells to show cell-specific timing of response to a K_{ATP}-channel blocker (tolbutamide) may be due to increased activity of K_{ATP}-channels and impaired electrical activity (Ashcroft and Rorsman 2004). The cell-specific magnitude of response to KIC and tolbutamide in ß-cells from hyperglycemic mouse indicates that cell-specific timing and magnitude of the Ca^{2+} response are controlled by different mechanisms.

β-Cells from type 2 diabetic subjects show a delayed Ca^{2+} response to glucose due to metabolic disturbances, but they react with a normal lag-time when challenged with arginine or sulfonylureas (Del Guerra *et al* 2005, Zaitsev *et al* 1997). β-Cells from *db/db* mice in fact responded to tolbutamide and arginine with a shorter lag-time than lean mouse β-cells and a similar tendency was found also in *ob/ob* mouse β-cells. It may be that chronic hyperglycemia slows down the metabolic rate but increases the sensitivity of K^+_{ATP} or Ca^{2+} channels (Kato *et al* 1996).

The timing of Zn^{2+} outflow recorded during the first stimulation with tolbutamide in lean mouse ß-cells correlated with the timing of calcium response recorded during the second stimulation. We showed that ß-cells repeat their calcium response pattern during consecutive stimulations with tolbutamide. It has also been found that cytoplasmic calcium changes and Zn^{2+} release are linked with regard to both timing and magnitude (Quan *et al* 2004, Wollheim and Pozzan 1984). We therefore conclude that the timing of insulin release during consecutive stimulations is cell-specific in cells from lean mice. No such correlation was found in *ob/ob* mouse ß-cells.

ß-Cells within intact islets showed cell-specific timing of their calcium responses. Fast responding ß-cells therefore may have a pacemaker function. It was recently claimed that ß-cells within an islet show identical temporal responses (Kuznetsov *et al* 2005). We could identify fast and slowly responding cells both in lean and *ob/ob* mouse islets. The variation was rather small in lean mouse islets, but in *ob/ob* mouse islets the range of lag-times was almost as large as in isolated ß-cells. This could be due to a disturbed stimulus-secretion coupling or to a damage of cell contacts and may explain the disorganization of calcium oscillations found in *ob/ob* mouse islets (Ravier *et al* 2002). We cannot exclude that part of the variation in lag-time could be caused by the handling of the tissue during the islet isolation procedure. ß-Cells may vary in their functional characteristics within pancreatic islets, because they originate not from a single stem cell but from a

number of different low-differentiated precursors (Lechner and Habener 2003). We have previously reported that intact islets, as a whole, show a specific response. Taken together, this indicates that both the cell specificity of each ß-cell and the functional connection between cells is important for islet-specific behaviour and adequate insulin release.

In Paper V, we could now show that there is a correlation between mitochondrial mass before the stimulation and the timing of the ß-cell cytoplasmic calcium response. This was done using Mitotracker Red and Fluo-3. There may be several mechanisms by which the mitochondrial state influences the timing of calcium response. Firstly, mitochondria are the main source of production of ATP, which plays a key role in pancreatic ß-cell glucose signalling. Secondly, before the generation of ATP from the glucose molecule, ATP is required for glucose phosphorylation to yield glucose-6-phosphate and fructose-2,6-bisphosphate. It has been suggested that these reactions depend on sufficient ß-cell ATP content prior to the glucose challenge (Ortsäter et al 2002). As a consequence, a large amount of active mitochondria could enhance the glycolysis. Thus, a larger mitochondrial mass can provide a higher rate of both glycolytic and mitochondrial metabolism. It is difficult to say which metabolic step is more important with regard to determining the lag time for calcium rise. The role of glycolytic vs. mitochondrial metabolism in glucose-stimulated insulin secretion is controversial. Mertz et al (1996) found that glycolytic ATP alone can sustain glucose-induced insulin release, but Ortsäter et al (2002) found that glycolysis alone could neither initiate nor maintain it. Mitochondrial metabolism may stimulate insulin release also through other mechanisms (Maechler and Wollheim 2001, MacDonald et al 2005).

The mitochondrial Ca^{2+} uptake, following the rise in cytoplasmic Ca^{2+} (Rutter et al 1993) may activate mitochondrial metabolism (Ainscow and Rutter 2001, Rutter et al 1996), providing a mitochondrial potentiation, which may have an important role in the response of islets to glucose. ATP is important for many processes in stimulated ß-cells, such as sequestration of Ca^{2+} before the $[Ca^{2+}]_i$ rise (19), insulin granular movement and the exocytotic process (Wollheim et al 1996). Decreased ATP levels result in opening of K_{ATP} channels (Kohler et al 1998). ATP is also suggested to be a secreted messenger in communication between ß-cells (Hellman et al 2004).

As our results from Paper III show, the cell specificity of mitochondrial metabolism is blunted in ß-cells from hyperglycemic mice in a way that affects timing of response but not the magnitude. There was no correlation between mitochondrial mass and the magnitude of calcium response. As it was suggested above, it is possible, that other factors, such a number and opening state of voltage-dependent calcium channels have a large influence on the magnitude of calcium rise. There may also be a technical explanation for this. Changes in $[Ca^{2+}]_i$ are indicated by changes in the absolute values for Fluo-3 fluorescence. Because of the dye degradation and leakage, such a system is more subject to experimental variation, when compared with ratiometric measurements, such as with fura-2. An existing correlation between mitochondrial mass and $[Ca^{2+}]_i$ peak height may therefore be difficult to detect using Fluo-3.

According to electron microscopy studies, ß-cells from 3-5-month-old *ob/ob* mice have fewer and larger mitochondria than lean mouse ß-cells (Diani *et al* 2004). Other studies have not found such differences (Jörns *et al* 1997). It has been suggested that β-cell dysfunction results from prolonged exposure to high glucose and elevated free fatty acid levels, leading to oxidative stress and apoptosis (Evans *et al* 2003). *ob/ob* Mice are hyperglycaemic, but we did not find differences in the localization of mitochondria or MitoTracker staining intensity when compared with ß-cells from normoglycemic mice. As shown previously (Paper II and III), the timing of the Ca^{2+} response to glucose did not differ between ß-cells from lean and *ob/ob* mice.

Calcium rise was less pronounced in the central cell areas, where most mitochondria were localized. This is not unexpected since calcium rise is caused by Ca^{2+} influx through plasma membrane channels. It supports the hypothesis that mitochondrial calcium uptake also has an impact on the cytoplasmic calcium signal (Duchen 2004). Thereby the activity of calcium-dependent processes may be partly regulated by mitochondria. It could also reflect that mitochondrial activation requires a smaller calcium increase than exocytosis does.

Voltage-dependent calcium channels are localized to specific membrane domains, so called "hot spots" (Qian and Kennedy 2001). We found no evidence that calcium increases occur in areas close to aggregates of mitochondria. Our data therefore suggest that hot spots are not connected to localised increases in ATP production.

Cells within the intact islet of Langerhans may function as a metabolic syncytium, secreting insulin in a coordinated and oscillatory manner in response to external fuel (Pipeleers 1987). Since the pacemakers in the islets are likely to be the cells with the shortest lag-times, there could be a possibility of identifying pacemaker cells within an islet on the basis of a larger mitochondrial mass. However, we saw no correlation between the MitoTracker intensity and the lag-times in most islets. With Fluo-3, we studied only the outer cells in the islet. For all we know, the signal propagation may not be radial (from a single source) and the source of propagation may be located near the surface of the islet. The range of lag-times between individual ß-cells is very narrow in lean mouse islets, which makes it difficult to detect a correlation. In one *ob/ob* mouse islet, ß-cells with a higher amount of active mitochondria responded to stimulation with a shorter lag-time. Synchronicity in *ob/ob* mouse islets is lower than in normal mouse islets. This may be attributed to an impaired cell coupling (Raviet *et al* 2002), but there is also a disturbed cell specificity of the response to mitochondrial stimulation.

High concentrations of MitoTracker (µM) may reduce mitochondrial respiration, but only a small effect was observed at the low concentration range (Buckman *et al* 2001). Other studies suggest that prolonged exposure to low concentrations of MitoTracker has little or no effect on mitochondrial function (Waters and Smith 2003).

Thus, we found that mitochondrial mass varied considerably between ß-cells and that mitochondrial mass was related to the timing of calcium response in both lean and *ob/ob* mouse ß-cells. The state of mitochondria before the stimulation

seems to determine the timing of secretory response and may be an important part of the explanation for the heterogeneity of ß-cell response.

Normal ß-cells show cell specific responses to all tested stimuli. ß-Cells from hyperglycemic mice have cell-specific timing and magnitude of responses to glucose and glyceraldehyde, but they show no temporal cell specificity when stimulated with a mitochondrial substrate. This suggests an altered mitochondrial function. The loss of cell-specific timing of response also at the step of calcium channel opening suggests that the mechanism(s) for setting the individual response characteristics is impaired in diabetic mouse ß-cells. Temporal cell specificity for all steps of the stimulus-secretion coupling may therefore be important for normal function. The timing of response in ß-cells may be controlled by their mitochondrial state.

SUMMARY

1. The heterogeneity of ß-cell responses is based on unique and reproducible characteristics of ß-cells.

2. Cell specificity of the ß-cell response is found in different rodent models. Aggregated ß-cells also show cell-specific responses.

3. Normal ß-cells show cell-specific Ca^{2+} responses when stimulated at different steps of the stimulus-secretion coupling. This means that not only the stimulus-secretion coupling, as a whole, is cell-specific but also different parts of it, such as mitochondrial metabolism, glycolysis and ion channel function.

4. ß-Cells from hyperglycemic mice show cell-specific timing and magnitude of responses to glucose and glyceraldehyde but they lose cell specificity of the timing when stimulated with a mitochondrial substrate or with depolarizing agents. This indicates that the mechanism(s) for setting the individual response characteristics is impaired in diabetic mouse ß-cells. This may be due to the altered functions of calcium channels and mitochondria. Cell specificity for all steps of the stimulus-secretion coupling may be necessary for normal ß-cell function.

5. ß-Cells with a larger number of active mitochondria react faster to stimulation. The lag-time for calcium rise may be determined by the mitochondrial state.

ACKNOWLEDGEMENTS

I wish to express my deepest gratitude to all colleagues and friends at the Department of Integrative Medical Biology, Umeå University, who create an enjoyable working atmosphere. In particular, I want to thank the following persons.

Professor Per Lindström, my supervisor, for all of his excellent guidance, optimism, his deep knowledge and willingness to share it, and for his patience in reading draft after draft of every paper, proposal and idea I wrote up.

Professor Janove Sehlin, my co-supervisor, for giving me this opportunity to make this PhD and for instruction in the ways of the research world. He has helped me to solve many problems and provided invaluable advice on how to improve my experiments as well as the thesis. I am very grateful for his support and personal concern.

Gerd Larsson-Nyrén, also my co-supervisor, who guided my work from my first days in diabetes research, for her enthusiasm, ability to generate ideas and for always supporting me. Also for being my travel companion at Post-EASD Islet Group Meetings.

Professor Andrey Zashikhin, for first introducing me to the field of histology research and his invaluable guidance during postgraduate years in Northern State Medical University in Russia.

Eva Hallin, for teaching me the laboratory technique and many times helping me out with the experiments. Her friendship and generous support during all these years have been invaluable.

I am grateful to all laboratory assistants in our department who have always been ready to give help or find things when I needed them: Gunilla Forsgren, Eva Boström, Karin Grabbe, Ann-Charlotte Idahl, Barbro Borgström, and Eva-Maj Lindström.

Doris Johansson, Thomas Jonsson and Mats Högström, for taking good care of the animals and fine selection of mice for the experiments, and also for always being considerate.

Anita Dreyer Perkiömäki, our excellent secretary, who has helped me a great deal with organising things and other practical matters.

My colleagues and friends in the department: Professor Ingrid Strömberg, Sara af Bjerken, Åsa Stenberg, Anna Nilsson and Martin Lundblad, for their support and friendly concern; Mattias Olsson for his valuable hints concerning the confocal microscope; Elisabet Berglöf, with whom we took a course in Stockholm; Per-Arne Oldenborg for interesting discussions and valuable suggestions; Franziska Marshinke, for being very supportive and helpful. Daniel Saiepour, with whom I shared an office, for being a nice company and interesting discussions.

Golbarg Abedi, for her collaboration in the fifth manuscript

Göran Dahlström, for the computer support.

Lev and Ludmila Novikov, for all the good advice.

My friends, Anna and Monika, who have been a great support, for sharing my ideas, thoughts and doubts; Yuri, for inspiring and amuzing scientific discussions; Elisabet, for first teaching me Swedish and for being a great companion during my first years in Umeå.

I am indebted to my parents, Vladimir and Ludmila, for their never ending support and love, for believing in me all these years no matter what I have chosen to do, and for planting in me the interest for science. I am grateful to my sister, Anya, for the encouragement and the joy she gives.

Anders, my unfailing source of love and support that I honestly think can get me through anything.

REFERENCES

Ainscow EK, Rutter GA. (2001) Mitochondrial priming modifies Ca^{2+} oscillations and insulin secretion in pancreatic islets. Biochem J. 353 (Pt 2), 175-180.

Aizawa T, Kaneko T, Yamauchi K, Yajima H, Nishizawa T, Yada T, Matsukawa H, Nagai M, Yamada S, Sato Y, Komatsu M, Itoh N, Hidaka H, Kajimoto Y, Hashizume K. (2001) Size-related and size-unrelated functional heterogeneity among pancreatic islets. Life Sci 69(22), 2627-2639.

Antunes CM, Salgado AP, Rosario LM, Santos RM. (2000) Differential patterns of glucose-induced electrical activity and intracellular calcium responses in single mouse and rat pancreatic islets. Diabetes 49(12), 2028-2038.

Ashcroft SJ, Ashcroft FM. (1992) The sulfonylurea receptor. Biochim Biophys Acta 1175(1), 45-59.

Ashcroft F, Rorsman P. (2004) Type 2 diabetes mellitus: not quite exciting enough? Hum Mol Genet 13 Spec No 1, R21-R31.

Aslanidi OV, Mornev OA, Vesterager M, Sorensen MP, Christiansen PL. (2002) A model for glucose-induced wave propagation in pancreatic islets of Langerhans. J Theor Biol 215, 273-286.

Berglund O, Frankel BJ, and Hellman B. (1978) Development of the insulin secretory defect in genetically diabetic (*db/db*) mouse. Acta Endocrinologica 87, 548-551.

Berglund O. (1980) Different dynamics of insulin secretion in the perfused pancreas of mouse and rat. Acta Endocrinol 93, 54–60.

Berglund O, Sehlin J, and Taljedal IB. (1984) Phosphate flush and glucose metabolism in pancreatic islets of young and old diabetic mice (C57BL/KsJ-*db/db*). Acta Endocrinol (Copenh) 105, 539-544.

Bergsten P, Grapengiesser E, Gylfe E, Tengholm A and Hellman B. (1994) Synchronous oscillations of cytoplasmic Ca^{2+} and insulin release in glucose-stimulated pancreatic islets. J Biol Chem 269, 8749-8753.

Bergsten P. (2000) Pathophysiology of impaired pulsatile insulin release. Diabetes Metab Res Rev. 16(3), 179-91.

Bokvist K, Eliasson L, Ammala C, Renstrom E, Rorsman P. (1995) Co-localization of L-type Ca^{2+} channels and insulin-containing secretory granules and its significance for the initiation of exocytosis in mouse pancreatic B-cells. EMBO J 14, 50-57.

Buckman JF, Hernandez H, Kress GJ, Votyakova TV, Pal S, Reynolds IJ. (2001) MitoTracker labeling in primary neuronal and astrocytic cultures: influence of mitochondrial membrane potential and oxidants. J Neurosci Methods 104, 165-176.

Calles-Escandon J, Robbins DC. (1987) Loss of early phase of insulin release in humans impairs glucose tolerance and blunts thermic effect of glucose. Diabetes 36(10), 1167-72.

Cerasi E, Luft R. (1967) What is inherited? What is added? Hypothesis for the pathogenesis of diabetes mellitus. Diabetes 16, 615–627.

Cerasi E, Luft R, Efendic S. (1972) Decreased sensitivity of the pancreatic ß cells to glucose in prediabetic and diabetic subjects. A glucose dose-response study. Diabetes 21, 224–234.

Charles S, Tamagawa T, Henquin J-C. (1982) A single mechanism for the stimulation of insulin release and 86Rb+ efflux from rat islets by cationic amino acids. Biochem J. 301-308.

Chen H, Charlat O, Tartaglia LA, Woolf EA, Weng X, Ellis SJ, Lakey ND, Culpepper J, Moore KJ, Breitbart RE, Duyk GM, Tepper RI, and Morgenstern JP. (1996) Evidence that

the diabetes gene encodes the leptin receptor: identification of a mutation in the leptin receptor gene in *db/db* mice. Cell 84, 490-495.

Cook DL. (1984) Electrical pacemaker mechanisms of pancreatic islet cells. Fed Proc 43, 2368–2372.

Curry DL, Bennett LL, Grodsky GM. (1968) Dynamics of insulin secretion by the perfused rat pancreas. Endocrinology 83, 572-584.

Deeney JT, Prentki M, Corkey BE. (2000) Metabolic control of beta-cell function. Semin Cell Dev Biol 11, 267-75.

Del Guerra S, Lupi R, Marselli L, Masini M, Bugliani M, Sbrana S, Torri S, Pollera M, Boggi U, Mosca F, Del Prato S, Marchetti P. (2005) Functional and molecular defects of pancreatic islets in human type 2 diabetes. Diabetes 54, 727-35.

Diani AR, Sawada G, Wyse B, Murray FT, Khan M. (2004) Pioglitazone preserves pancreatic islet structure and insulin secretory function in three murine models of type 2 diabetes. Am J Physiol Endocrinol Metab 286, E116-E122.

Duchen MR. (2004) Roles of mitochondria in health and disease. Diabetes 53, S96-S102.

Dunne M. (1990) Nutrient and pharmacological stimulation of insulin-secreting cells: marked differences in the onset of electrical activity. Exp Physiol 75, 771–777.

Dunne MJ, Petersen OH. (1991) Potassium selective ion channels in insulin-secreting cells: physiology, pharmacology and their role in stimulus-secretion coupling. Biochim Biophys Acta 1071, 67-82.

Evans JH and Sanderson MJ. (1999) Intracellular calcium oscillations induced by ATP in airway epithelial cells. Am J Physiol Lung Cell Mol Physiol 277, L30–L41.

Evans JL, Goldfine ID, Maddux BA, Grodsky GM. (2003) Are oxidative stress-activated signaling pathways mediators of insulin resistance and beta-cell dysfunction? Diabetes 52 1-8.

Faehling M, Ashcroft FM. (1997)Heterogeneity of ß-cell secretion. Possible involvement of K-ATP channels. Adv Exp Med Biol 426, 247-252.

Frederickson CJ and Bush AI (2001). Synaptically released zinc: physiological functions and pathological effects. Biometals 14, 353–366.

Gee KR, Zhou ZL, Qian WJ, Kennedy R. (2002) Detection and imaging of zinc secretion from pancreatic beta-cells using a new fluorescent zinc indicator. J Am Chem Soc 124, 776-778.

Gilon P, Jonas JC, Henquin JC. (1994) Culture duration and conditions affect the oscillations of cytoplasmic calcium concentration induced by glucose in mouse pancreatic islets. Diabetologia 37, 1007-1014.

Grapengiesser E, Gylfe E, Hellman B. (1999) Synchronization of glucose-induced Ca^{2+} transients in pancreatic ß-cells by a diffusible factor. Biochem Biophys Res Commun 254, 436-439.

Grill V, Adamson U, Cerasi E. (1978) Immediate and time-dependent effects of glucose on insulin release from rat pancreatic tissue. Evidence for different mechanisms of action. J Clin Invest 61, 1034-1043.

Grodsky GM, Curry D, Landahl H, Bennett L. (1969) [Further studies on the dynamic aspects of insulin release in vitro with evidence for a two-compartmental storage system] Acta Diabetol Lat 6 Suppl 1, 554-578.

Grynkiewicz G, Poenie M, Tsien RY.(1985) A new generation of Ca2+ indicators with greatly improved fluorescence properties. J Biol Chem 260, 3440-3450.

Gunawardana SC, Sharp GW. (2002) Intracellular pH plays a critical role in glucose-induced time-dependent potentiation of insulin release in rat islets. Diabetes 51, 105-113.

Gylfe E. (1989) Glucose-induced buffering of cytoplasmic Ca2+ in the pancreatic beta-cell--an artifact or a physiological phenomenon? Biochem Biophys Res Commun 159, 907-912.

Gylfe E, Grapengiesser E, and Hellman B. (1991) Propagation of cytoplasmic Ca 2+ oscillations in clusters of pancreatic ß-cells exposed to glucose. Cell Calcium 12, 229–240.

Halaas JL, Gajiwala KS, Maffei M, Cohen SL, Chait BT, Rabinowitz D, Lallone RL, Burley SK, Friedman JM. (1995) Weight-reducing effects of the plasma protein encoded by the obese gene. Science 269(5223), 543-546.

Hahn HJ, Hellman B, Lernmark A, Sehlin J, Taljedal IB. (1974) The pancreatic ß-cell recognition of insulin secretogogues. Influence of neuraminidase treatment on the release of insulin and the islet content of insulin, sialic acid, and cyclic adenosine 3':5'-monophosphate. J Biol Chem 249, 5275-5284.

Heding LG. (1966) A simplified insulin radioimmunoassay, in: L. Donato, G. Milhaud, G. Sirchis (Eds.), Labelled Proteins in Tracer Studies, Euratom, Brussels, pp. 345–351.

Hellerström, C, Petersson B, and Hellman B. (1960) Some properties of the B cells in the islets of Langerhans studied with regard to the position of the cells. Acta Endocrinol 34, 449-456.

Hellman B. (1965) Studies in obese-hyperglycemic mice. Ann N Y Acad Sci 131, 541-558.

Hellman B, Idahl LA, Lernmark A, Sehlin J, Taljedal IB. (1974) The pancreatic ß-cell recognition of insulin secretagogues. Comparisons of glucose with glyceraldehyde isomers and dihydroxyacetone. Arch Biochem Biophys 162, 448-457.

Hellman B, Dansk H, Grapengiesser E. (2004) Pancreatic ß-cells communicate via intermittent release of ATP. Am J Physiol Endocrinol Metab. 286, E759-E765.

Herchuelz A, Lebrun P, Boschero AC, Malaisse WJ. (1984) Mechanism of arginine-stimulated Ca^{2+} influx into pancreatic B cell. Am J Physiol 246 (1 Pt 1) E38-E43.

Herchuelz A, Pochet R, Pastiels C, Van Praet A. (1991) Heterogeneous changes in $[Ca^{2+}]_i$ induced by glucose, tolbutamide and K^+ in single rat pancreatic B cells. Cell Calcium 12, 577–586.

Hiriart M, Ramirez-Medeles MC. (1991) Functional subpopulations of individual pancreatic B-cells in culture. Endocrinology 128, 3193-3198.

Hunt CE, Lindsey JR, Walkley SU. (1976) Animal models of diabetes and obesity, including the PBB/Ld mouse. Federation Proceedings 35, 1206-1217.

Idahl LA and Lembert N. (1995) Glycerol 3-phosphate-induced ATP production in intact mitochondria from pancreatic B-cells. Biochem J 312 (Pt 1), 287-292.

Ingalls A, Dickie MM, Snell GD (1950) Obese, a new mutation in the house mouse. J. Hered 51, 317-318.

Int Veld PA, Pipeleers DG, Gepts W. (1986) Glucose alters configuration of gap junctions between pancreatic islet cells. Am J Physiol 251(2 Pt 1), C191-C196.

Jonas JC, Gilon P, Henquin JC. (1998) Temporal and quantitative correlations between insulin secretion and stably elevated or oscillatory cytoplasmic Ca^{2+} in mouse pancreatic beta-cells. Diabetes 47, 1266-1273.

Jonkers FC, Jonas JC, Gilon P, Henquin JC. (1999) Influence of cell number on the characteristics and synchrony of Ca^{2+} oscillations in clusters of mouse pancreatic islet cells. J Physiol 520 Pt 3, 839-49.

Jonkers FC, Guiot Y, Rahier J, Henquin JC. (2001) Tolbutamide stimulation of pancreatic beta-cells involves both cell recruitment and increase in the individual Ca(2+) response. Br J Pharmacol 133, 575-585.

Jörns A, Munday R, Tiedge M, Lenzen S. (1997) Comparative toxicity of alloxan, N-alkylalloxans and ninhydrin to isolated pancreatic islets in vitro. J. Endocrinol. 155, 283−293.

Kato S, Ishida H, Tsuura Y, Tsuji K, Nishimura M, Horie M, Taminato T, Ikehara S, Odaka H, Ikeda I, Okada Y, Seino Y. (1996) Alterations in basal and glucose-stimulated voltage-dependent Ca2+ channel activities in pancreatic beta cells of non-insulin-dependent diabetes mellitus GK rats. J Clin Invest 97, 2417-25.

Kay AR. (2004) Detecting and minimizing zinc contamination in physiological solutions. BMC Physiol 4, 4.

Kiekens R, In't Veld P, Mahler T, Schuit F, Van De Winkel M, Pipeleers D. (1992) Differences in glucose recognition by individual rat pancreatic B cells are associated with intercellular differences in glucose-induced biosynthetic activity. J Clin Invest 89, 117-125.

Kinard TA, de Vries G, Sherman A, and Satin LS. (1999) Modulation of the bursting properties of single mouse pancreatic ß-cells by artificial conductances. Biophys J 76, 1423–1435.

Kohler M, Norgren S, Berggren PO, Fredholm BB, Larsson O, Rhodes CJ, Herbert TP, Luthman H. (1998) Changes in cytoplasmic ATP concentration parallels changes in ATP-regulated K+-channel activity in insulin-secreting cells. FEBS Lett. 441 97-102.

Kuznetsov A, Bindokas VP, Marks JD, Philipson LH. (2005) FRET-based voltage probes for confocal imaging: membrane potential oscillations throughout pancreatic islets. Am J Physiol Cell Physiol 289, C224 - C229.

Larsson-Nyrén G and Sehlin J. (1996) Comparison of the effects of perchlorate and Bay K 8644 on the dynamics of cytoplasmic Ca^{2+} concentration and insulin secretion in mouse ß-cells. Biochem J 314, 167–173.

Lechner A, Habener JF. (2003) Stem/progenitor cells derived from adult tissues: potential for the treatment of diabetes mellitus. Am J Physiol Endocrinol Metab 284, E259-E266.

Lembert, N., Idahl, L.A. (1998) Alpha-ketoisocaproate is not a true substrate for ATP production by pancreatic beta-cell mitochondria. Diabetes 47, 339-344.

Lenzen S, Lerch M, Peckmann T, Tiedge M. (2000) Differential regulation of $[Ca^{2+}]_i$ oscillations in mouse pancreatic islets by glucose, alpha-ketoisocaproic acid, glyceraldehyde and glycolytic intermediates. Biochim Biophys Acta 1523, 65-72.

Lernmark Å. (1974) The preparation of and studies on free cell suspensions from mouse pancreatic islets, Diabetologia 10, 431–438.

Levy J, Malaisse WJ. (1975) The stimulus-secretion coupling of glucose-induced insulin release. XVII. Effects of sulfonylureas and diazoxide on insulin biosynthetic activity. Biochem Pharmacol 24, 235–239.

Lindstrom P, Sehlin J, Frankel BJ. (1996) Glucose-stimulated elevation of cytoplasmic calcium is defective in the diabetic Chinese hamster islet B cell. Eur J Endocrinol, 134(5), 617-625.

Lund PE, Gylfe E, Hellman B. (1989) Leucine induces initial lowering of cytoplasmic Ca^{2+} in pancreatic ß-cells without concomitant inhibition of insulin release. Biochem Int 19(1), 83-87.

MacDonald MJ. (1989) Does glyceraldehyde enter pancreatic islet metabolism via both the triokinase and the glyceraldehyde phosphate dehydrogenase reactions? A study of these enzymes in islets.Arch Biochem Biophys. 270(1), 15-22.

MacDonald MJ, Fahien LA, Brown LJ, Hasan NM, Buss JD, Kendrick MA. (2005) Perspective: emerging evidence for signaling roles of mitochondrial anaplerotic products in insulin secretion. Am J Physiol Endocrinol Metab 288, E1-E15.

Maechler P and Wollheim CB. (2001) Mitochondrial function in normal and diabetic beta-cells. Nature 414, 807-812.

Malaisse WJ. (1993) Is type 2 diabetes due to a deficiency of FAD-linked glycerophosphate dehydrogenase in pancreatic islets? Acta Diabetol 30, 1-5.

Marie JC, Bailbe D, Gylfe E and Portha B. (2001) Defective glucose-dependent cytosolic Ca^{2+} handling in islets of GK and nSTZ rat models of type 2 diabetes. J Endocrinol 169, 169-176.

Matschinsky FM. (1996) Banting Lecture 1995. A lesson in metabolic regulation inspired by the glucokinase glucose sensor paradigm. Diabetes 45(2), 223-241.

Meda P, Denef JF, Perrelet A, and Orci L. (1980) Nonrandom distribution of gap junctions between pancreatic ß-cells. Am J Physiol Cell Physiol 238, C114–C119.

Mertz RJ, Worley JF, Spencer B, Johnson JH, Dukes ID. (1996) Activation of stimulus-secretion coupling in pancreatic beta-cells by specific products of glucose metabolism. Evidence for privileged signaling by glycolysis. J Biol Chem. 271, 4838-4845.

Misler S, Barnett DW, Pressel DM, Gillis KD, Scharp DW, Falke LC. (1992) Stimulus-secretion coupling in ß-cells of transplantable human islets of Langerhans. Evidence for a critical role for Ca2+ entry. Diabetes 41(6), 662-670.

Munari-Silem Y, Rousset B. (1996) Gap junction-mediated cell-to-cell communication in endocrine glands--molecular and functional aspects, a review. Eur J Endocrinol 135(3), 251-264.

Nadal A, Quesada I, Soria B. (1999) Homologous and heterologous asynchronicity between identified alpha-, ß- and delta-cells within intact islets of Langerhans in the mouse. J Physiol 517 (Pt 1), 85-93.

Nesher R, Eylon L, Segal N, Cerasi E. (1989) ß-cell memory to insulin secretagogues, characterization of the time-dependent inhibitory control system in the isolated rat pancreas.Endocrinology. 124(1), 142-148.

Newgard CB, McGarry JD. (1995) Metabolic coupling factors in pancreatic ß-cell signal transduction. Annu Rev Biochem 64, 689-719.

Nilsson T, Arkhammar P, Berggren PO. (1988) Dual effect of glucose on cytoplasmic free Ca^{2+} concentration and insulin release reflects the ß-cell being deprived of fuel. Biochem Biophys Res Commun 153, 984-991.

Orci L, Unger RH, Renold AE. (1973) Structural coupling between pancreatic islet cells. Experientia 29(8), 1015-1018.

Ortsäter H, Liss P, Akerman KE, Bergsten P. (2002) Contribution of glycolytic and mitochondrial pathways in glucose-induced changes in islet respiration and insulin secretion. Pflugers Arch. 444, 506-512.

Palti Y, David GB, Lachov E, Mida YH, Schatzberger R. (1996) Islets of Langerhans generate wavelike electric activity modulated by glucose concentration. Diabetes 45(5), 595-601.

Panten U. (1975) Effects of alpha-ketomonocarboxylic acids upon insulin secretion and metabolism of isolated pancreatic islets. Naunyn Schmiedebergs Arch Pharmacol 291, 405-420.

Pe´rez-Armendariz E, Atwater I, and Bennett MVL. (1995) Mechanisms for fast intercellular communication within a single islet of Langerhans. In, Pacemaker Activity and Intracellular Communication, edited by Huizinga JD. Boca Raton, FL, CRC, p. 305–321.

Pipeleers D. (1987) The biosociology of pancreatic B cells. Diabetologia 30, 277-291.

Pipeleers DG, Kiekens R, Ling Z, Wilikens A, Schuit F. (1994) Physiologic relevance of heterogeneity in the pancreatic beta-cell population. Diabetologia 37 (Suppl. 2), S57-S64.

Polonsky KS, Given BD, Hirsch LJ, Tillil H, Shapiro ET, Beebe C, Frank BH, Galloway JA, Van Cauter E. (1998) Abnormal patterns of insulin secretion in non-insulin-dependent diabetes mellitus. N Engl J Med 318, 1231–1239.

Pralong WF, Bartley C, Wollheim CB. (1990) Single islet ß-cell stimulation by nutrients: relationship between pyridine nucleotides, cytosolic Ca^{2+} and secretion. EMBO J 9(1), 53-60.

Qian WJ, Kennedy RT. (2001) Spatial organization of $Ca(^{2+})$ entry and exocytosis in mouse pancreatic ß-cells. Biochem. Biophys. Res. Commun. 286, 315-321.

Qian WJ, Gee KR, Kennedy RT.(2003) Imaging of Zn^{2+} release from pancreatic beta-cells at the level of single exocytotic events. Anal Chem 75, 3468-75.

Qian WJ, Peters JL, Dahlgren GM, Gee KR, Kennedy RT. (2004) Simultaneous monitoring of Zn^{2+} secretion and intracellular Ca^{2+} from islets and islet cells by fluorescence microscopy. Biotechniques 37, 922-924, 926, 928-30 passim.

Ravier MA, Sehlin J, Henquin JC. (2002) Disorganization of cytoplasmic Ca^{2+} oscillations and pulsatile insulin secretion in islets from ob/ ob mice. Diabetologia 45(8), 1154-63

Roe MW, Philipson LH, Frangakis CJ, Kuznetsov A, Mertz RJ, Lancaster ME, Spencer B, Worley JF 3rd, and Dukes ID. (1994) Defective glucose-dependent endoplasmic reticulum Ca^{2+} sequestration in diabetic mouse islets of Langerhans. J Biol Chem 269, 18279-18282

Roe MW, Worley JF 3rd, Tokuyama Y, Philipson LH, Sturis J, Tang J, Dukes ID, Bell GI, Polonsky KS. (1996) NIDDM is associated with loss of pancreatic beta-cell L-type Ca^{2+} channel activity. Am J Physiol. 270 (Pt 1), E133-E140.

Rooney TA, Sass EJ, and Thomas AP. (1989) Characterization of cytosolic calcium oscillations induced by phenylephrine and vasopressin in single Fura-2-loaded hepatocytes. J Biol Chem 264, 17131–17141.

Rutter GA, Theler JM, Murgia M, Wollheim CB, Pozzan T, Rizzuto R. (1993) Stimulated Ca^{2+} influx raises mitochondrial free Ca^{2+} to supramicromolar levels in a pancreatic beta-cell line. Possible role in glucose and agonist-induced insulin secretion. J Biol Chem. 268, 22385-22390.

Rutter GA, Burnett P, Rizzuto R, Brini M, Murgia M, Pozzan T, Tavare JM, Denton R M. (1996) Subcellular imaging of intramitochondrial Ca^{2+} with recombinant targeted aequorin: significance for the regulation of pyruvate dehydrogenase activity. Proc Natl Acad Sci U.S.A. 93, 5489-5494.

Salomon D and Meda P. (1986) Heterogeneity and contact-dependent regulation of hormone secretion by individual B cells. Exp Cell Res 162, 507–520.

Schatz H, Maier V, Nierle C, Pfeiffer EF. (1972) The effect of tolbutamide and glibenclamide on the incorporation of [3 H]leucine and on the conversion of proinsulin to insulin in isolated pancreatic islets. FEBS Lett 26, 237–40.

Schuit FC, Int Veld PA, Pipeleers DG. (1988) Glucose stimulates proinsulin biosynthesis by a dose-dependent recruitment of pancreatic ß cells. Proc Natl Acad Sci U S A 85, 3865-3869.

Schuit FC, De Vos A, Moens K, Quartier E, Heimberg H. (1997) Glucose-induced B-cell recruitment and the expression of hexokinase isoenzymes. Adv Exp Med Biol 426, 259-266.

Stauffacher W, Lambert AE, Vecchio D, Renold AE. (1967) Measurements of insulin activities in pancreas and serum of mice with spontaneous ("Obese" and "New Zealand

Obese") and induced (Goldthioglucose) obesity and hyperglycemia, with considerations on the pathogenesis of the spontaneous syndrome. Diabetologia 3, 230-237.

Stauffacher W, Renold AE. (1969) Effect of insulin in vivo on diaphragm and adipose tissue of obese mice. Am J Physiol 216, 98-105.

Stefan Y, Meda P, Neufeld M, and Orci L. (1987) Stimulation of insulin secretion reveals heterogeneity of pancreatic B cells in vivo. J Clin Invest 80, 175–183.

Tamarit-Rodriguez J, Idahl LA, Gine E, Alcazar O, Sehlin J. (1998) Lactate production in pancreatic islets. Diabetes 47, 1219-1223.

Trube G, Rorsman P, Ohno-Shosaku T. (1986) Opposite effects of tolbutamide and diazoxide on the ATP-dependent K^+ channel in mouse pancreatic ß-cells. Pflugers Arch 407, 493-499.

Waters J, Smith SJ. (2003) Mitochondria and release at hippocampal synapses. Pflugers Arch 447, 363-370.

Wollheim CB, Pozzan T. (1984) Correlation between cytosolic free Ca^{2+} and insulin release in an insulin-secreting cell line. J Biol Chem 259, 2262-2267.

Wollheim CB, Lang J, Regazzi R (1996) The exocytotic process of insulin and its regulation by Ca^{2+} and G-proteins. Diabetes Rev. 4 276–297.

Van Schravendijk CF, Kiekens R, and Pipeleers DG. (1992) Pancreatic ß cell heterogeneity in glucose-induced insulin secretion. J Biol Chem 25, 21344–21348.

Yagodin S, Holtzclaw LA, Russell JT (1995) Subcellular calcium oscillators and calcium influx support agonist-induced calcium waves in cultured astrocytes. Mol Cell Biochem 149-150, 137-144.

Zaitsev S, Efanova I, Ostenson CG, Efendic S, and Berggren PO. (1997) Delayed Ca^{2+} response to glucose in diabetic GK rat. Biochem Biophys Res Commun 239, 129-133.